A Thesis

entitled

Comparison of Electrospun and Solvent Cast PLA/PVA Inserts as Potential Ocular Drug Delivery Vehicles

by

Rajan Sharma Bhattarai

Submitted to the Graduate Faculty as partial fulfillment of the requirements for the

Master of Science Degree in Pharmaceutical Sciences

Industrial Pharmacy

_____

Sai Hanuman Sagar Boddu, PhD., Committee Chair

_____

Jerry Nesamony, PhD, Committee Member

_____

Sarit Bhaduri, PhD, Committee Member

_____

Amanda Bryant-Friedrich, PhD, Dean
College of Graduate Studies

The University of Toledo

August 2016

An Abstract of

Comparison of Electrospun and Solvent Cast PLA/PVA Inserts as Potential Ocular Drug Delivery Vehicles

by

Rajan Sharma Bhattarai

Submitted to the Graduate Faculty as partial fulfillment of the requirements for the Master of Science Degree in Pharmaceutical Sciences
Industrial Pharmacy

The University of Toledo

August 2016

Purpose: The purpose of this work was to develop, characterize and compare electrospun nanofiber inserts (ENIs) and solvent cast polymeric inserts for ocular drug delivery.

Methods: ENI and solvent cast inserts (SCIs) of dexamethasone were fabricated using a blend of poly-lactic acid (PLA) and poly-vinyl alcohol (PVA). Inserts contained 1%, 5% and 10% dexamethasone (by weight). Inserts were characterized for morphology, thickness, pH in simulated tear fluid (STF, pH 7.4), drug content, thermal analysis, infrared (IR) spectroscopy, *in vitro* drug release, dimethylformamide (DMF) and chloroform content and cytotoxicity in cultured bovine corneal endothelial cells. The inserts were sterilized by UV radiation for 10 minutes and tested for sterility using plate and direct inoculation techniques.

Results: The thickness of 1%, 5%, and 10% dexamethasone-loaded ENIs were found to be 50 μm, 62.5 μm, and 93.3 μm, respectively with good folding endurance. Inserts prepared using the solvent casting technique were brittle with thickness values greater than 200 μm. The release rate of dexamethasone from 1%, 5% and 10% ENIs were found to be 0.62 μg/h, 1.46 μg/h, and 2.30 μg/h respectively, while those from solvent cast technique

were erratic. A sustained release of dexamethasone was observed from 10% inserts for up to 36 hours. The quantities of DMF in ENIs and SCIs were found to be 0.007% w/w and 0.123% w/w, respectively. The chloroform content in both the inserts was below the detection limit. In addition, the inserts were sterilized by UV radiation and tested for sterility by direct inoculation in tubes and plate inoculation method in a petri dish. No cytotoxicity was observed from ENIs in cultured bovine corneal endothelial cells for up to 24 hours.

Conclusion: Based on the results obtained, we conclude that ENIs are better than inserts obtained by solvent casting technique and could be utilized as a potential delivery system for treating anterior segment ocular diseases.

Dedicated to my Family

Acknowledgements

I would like to acknowledge who have directly or indirectly contributed with their time and expertise to help me through the research work and come to this stage. I would like to appreciate Dr. Sai Boddu for taking me in his research team, and providing me with all the resources needed for completion of this research. His support, guidance and research insight have been the stepping stones over which this research work has been built. I would like to thank Dr. Jerry Nesamony for his instrumental support with HPLC, guidance and for being part of my defense committee. I would like to thank Dr. Sarit Bhaduri for collaborating with us on this project, providing the facility and expertise on electrospinning process and being part of my defense committee.

I express my gratitude to Dr. Kenneth Alexander for helping me throughout the course duration and providing me motivation when needed. I would like to thank Dr. Zahoor Shah, Dr. Panee Burkel, Dr. Pramod Paudel for technical support and allowing me to use their facility. I would like to thank Kastel's Slaughter House & Processing Center (Riga, MI) for providing bovine eyes for my study. This work was supported by the grant from the deArce Memorial Endowment Fund.

I am grateful and thankful to everyone who have helped me during my masters at a personal level or my research. I am thankful to my friends, Rami, Zahraa, Hasheem, Saugat, Ahmed, Rinda, Salam, Ameya, Padam, Pallabita for they have been instrumental in my success.

Table of Contents

List of Tables

List of Figures

Chapter 1

Introduction

1.1 Electrospinning and its history

Electrospinning is a process of forming micro/nanometer-sized polymeric fibers, either hollow or solid, with the application of the electric force on the polymeric solution at the tip of a conducting tube. It is one of the most commonly used techniques to obtain continuous fibers in the nanometer size range [1-3]. Electrospinning, also known as electrostatic spinning, has been extensively used for over three decades and its usefulness in the fields of science, technology is increasing with time.

The aerosols generated by the application of electric potential to the fluids were first described by Bose in 1745. Further, Lord Rayleigh studied the amount of charge needed by the fluid to overcome the surface tension of a drop. Cooley and Morton patented the first device to spray the liquids under the influence of electrical charge in 1902 and 1903, but the fabrication of the artificial silk was done by Hagiwaba et al., in 1929 [4]. The studies in the 1940s, 50s and 60s were limited and mainly focused on obtaining uniform size particle/fibers, decreasing the size, understanding and optimizing parameters and designing the instruments [5, 6]. In 1990s, the process was finally taken up by educational institutes

and since then many studies have been done on the versatility of manufacturing and application of the electrospun particles [2].

1.2 Process of electrospinning

The electrospinning process involves the use of a very high voltage source (either of positive or negative polarity) to charge the polymer solution or melt, a grounded collector and a syringe pump. It is advisable to perform the electrospinning process in a closed hood with minimal atmospheric influence, which serves as a safety measure for fibers and the personnel. When sufficient repulsive charge is accumulated and the repulsive force is equal to the surface tension, the drop surface on the conducting tube starts to form a cone called a Taylor cone. The conducting polymer solution/melt can exist in an equilibrium cone form under the influence of electric field in a semi-vertical angle of 49.3° [7]. If the electric field is increased further, surface tension is overcome by the repulsive force. This results in the formation of a liquid jet from the Taylor cone when there is sufficient attraction between the molecules in the solution/melt. If the solution doesn't have sufficient cohesive attraction, the jets break and the resulting particles are sprayed onto a collector plate. The fiber originating from the Taylor cone travels through the air towards the collector plate and during the process the solvent evaporates depositing a solid fiber on the collector plate [6, 7]. The schematic representation of the electrospinning process is shown in Figure 1.1. The jet starts to experience instability after travelling through the air for a short distance and then starts to bend into loops and thus increases the path distance to the collector. This process assists in fiber thinning and solvent evaporation. There are multiple theories proposed on the reason behind the jet instability. Some of the prominent theories include:

repulsive interaction of charges in the polymer jet [8]; increase in charge density during jet thinning, thus increasing radial charge repulsion to cause jet splitting at a critical charge density [9]; "whipping" instability (spiraling loops) [10] causing the fiber to turn, bend [11] and/or splay [12]. Shin et al. have suggested the whipping stability concept based on the results obtained using high-speed photography where single strand of jet whipped very fast to give a cone like appearance [11]. The "inverted cone" appearance had long been misunderstood as splitting of the jet midway through the travel in the air.

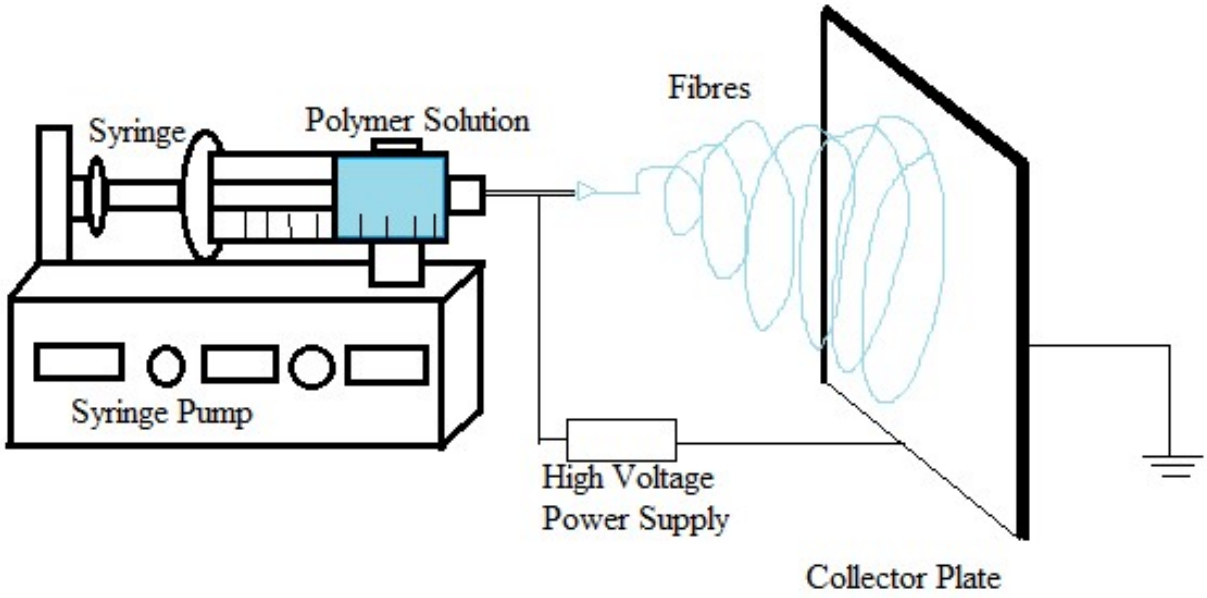

Figure 1.1: Schematic of electrospinning system. The system consists of polymer solution/melt in a syringe mounted on a syringe pump operating at a constant slow speed. High voltage DC supply is connected to the needle of the syringe to charge the fluid. With sufficient voltage the fluid forms a Tylor cone and then jet erupts from the cone towards the collector plate with whipping instability.

1.2.1 Physics of electrospinning

When the electric field/voltage is increased gradually and the surface of the drop becomes convex at a certain voltage, V_c (critical voltage) is reached. At V_c, the jets (electrospinning) and sprays (electrospraying) begins, which is represented by the equation 1.

$$V_c = 4\frac{H^2}{L^2}\left(Ln\frac{2L}{R} - \frac{3}{2}\right)(0.117\pi\gamma R) \quad \text{..... Eq. 1}$$

Where, H is separation between capillary and the collector, L is length of capillary, R is the radius of capillary and γ is the surface tension [7]. This relationship was identified by Taylor and similar relationship for the potential required for electrospraying of charged pendent drop of solutions from the pendant in a capillary tube was given by Hendrick et al. as given below in equation 2 [13, 14].

$$V = 300\sqrt{20\pi\gamma}\mathrm{r} \quad \text{..... Eq. 2}$$

Where, V is the required voltage, γ is the surface tension and r is the radius of the pendant drop. Even though viscosity and conductivity are vital in the electrospinning process, they are missing in the equation. The use of applied voltage and the surface tension gives a representative equation for slightly conducting, medium to low conductivity solutions [14].

1.3 Parameters of electrospinning

The electrospinning process is simple and does not involve heavy machinery. The processing parameters and solution parameters affect the size, porosity and uniformity of

the fibers. These parameters have been discussed individually; however, the observations made in any particular study by a team of researchers are not universal. The modification of a parameter in one polymer may produce a totally different result with another polymer. In addition, none of the parameters act independently during the electrospinning process and the final fibers are a result of a combination of several parameters.

1.3.1 Process related parameters of electrospinning

1.3.1.1 Applied Voltage

The primary factor influencing the formation of fibers is the strength of the applied DC voltage. The size of the fiber, formation of beads and absence of jet formation are all dependent on the applied DC voltage. With an increase in the applied voltage of polyethylene oxide (PEO) /water system, the originating site for the jet changes from the tip of the pendent drop to the tip of the capillary and the volume of the pendent drop decreases gradually (Figure 1.2). When the fiber is formed from within the capillary, the bead defects in the fiber increase [6, 15]. A reduction in voltage up to some range moves the splaying (instability) point towards the tip of the capillary i.e., jet becomes unstable earlier [12]. A study by Reneker and Chun reported no significant change in the fiber diameter with change in the electric field with PEO solution [16]. On the other hand, electrospun polyvinyl alcohol (PVA)/water solution exhibited a broad diameter distribution above 10 kV [17, 18]. In another study, Megelski et al. observed an increase in fiber size of polystyrene with decrease in spinning voltage and with no significant change in the pore formation in fibers [19].

The fibers formed during the electrospinning process, transport charge across to the grounded collector plate to close the circuit due to which the electric current associated

with the process can be measured. When conductivity, dielectric constant and flow rate through the pump remains the same, an increase in current indicates increase in mass of the fibers formed. During the electrospinning process, the increase in current is gradual at first and then goes up sharp from one voltage point while sharp step increases are observed during electrospraying. The point of sharp change in current could be indicative of the defect/change in the bead density [15].

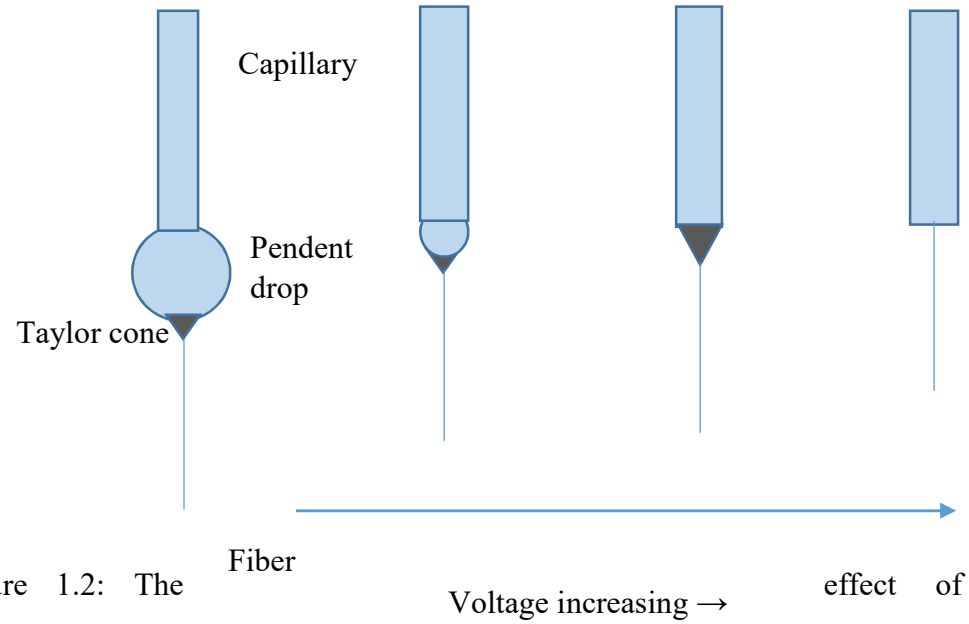

Figure 1.2: The effect of applied *Increasing Voltage gives initial decrease and then increase in fiber diameter*

electric field on Taylor cone formation (dark colored tip). At low electric field pendant drop is formed at the tip of the capillary and then a cone is formed on the tip. When the applied voltage is increased the drop size decreases till a cone is formed at the tip of the capillary. If the voltage is further increased, then the fiber is formed within the capillary.

1.3.1.2 Flow rate

The polymer flow rate has a direct impact on the size, shape and porosity of electrospun fibers. A study on polystyrene/tetrahydrofuran (THF) solutions by Megelki et al. reported an increase fiber diameter and pore size with flow rate. However, at high flow rates, bead defects and flat ribbon like structures were observed due to insufficient drying [19]. In a different study, similar effect on fiber morphology was observed with a 20 weight% solution of nylon 6 in formic acid at a constant electric field of 20 kV at a higher flow rate. An optimal flow rate of 0.5 ml/h resulted in fibers with narrowest fiber diameter distribution and stable Taylor cone. However, at low flow rates the Taylor cone could not be maintained and reduced over time to obtain fiber from within the capillary tip. At high flow rates of 1.0 ml/h and 1.5 ml/h, electric field was not sufficient to spin all the solution and only a few drops were sprayed as they broke off from the capillary due to the gravitational force [20].

1.3.1.3 Capillary – collector distance

The distance between the capillary and the collector plate is not as significant as the other factors. However, sometimes the distance needs to be optimized as it might be the factor that distinguishes electrospraying and electrospinning. According to Doshi and Reneker, the larger the distance from the Taylor cone the smaller the fiber diameter [9]. Jaegar et al. reported a decrease in fiber diameter (19 μm, 11 μm and 9 μm) with increasing distance (1 cm, 2 cm and 3.5 cm) from the orifice [12]. For the electrospun polystyrene polymer fiber, decreasing the distance between the capillary and collector from 35 cm to 30 cm led to the formation of non homogeneously distributed elongated beads [19].

1.3.2 Solution related parameters of electrospinning

1.3.2.1 Concentration of solution

Viscosity and surface tension, which determine the spinnability of a solution, should be taken into consideration in determining the concentration of solution/melt for electrospinning. Surface tension is a dominating factor in a low concentration solution (low viscosity, < 1 poise) and at such concentration; drops will be formed instead of a continuous fiber. At higher concentration (viscosity > 20 poise), the flow of the solution cannot be controlled and maintained. In the PEO/water study discussed above in Section 1.4.1, a concentration range of 4-10 wt % with viscosity and surface tension ranging between 1-20 poise and 55-35 dynes/cm, respectively were studied. At low concentrations of 4%, fibers were not sufficiently dry and formed fiber junctions and bundles. At higher concentrations, straight and cylindrical fibers with less fiber junction and bundles were reported. The diameter of the electrospun PEO fibers increased with concentration and a bimodal size distribution was observed above 7 wt % concentration. The average diameter of the fibers was reported to be related to solution concentration through the power law relationship with an exponent of 0.5 [15]. A statistical study by Sukigara et al. on regenerated silk proved that the silk concentration was the most important parameter in producing uniform fibers of diameter less than 100 nm [21]. In a different study, 15 and 20% w/v solutions of poly(desaminotyro-syl-tyrosine ethyl ester carbonate) (Poly(DTE carbonate)) were electrospun at a voltage level of 10 kV to 25 kV at 10 cm distance. Beaded fibers were observed during electrospinning at a lower concentration solution till 20 kV and the density of beads decreased till 15 kV; average fiber diameter increased from 20 kV to 25 kV. At

higher solution concentrations, the smooth fibers obtained showed an increasing diameter and decreasing fiber density with increase in electric field from 10 kV to 25 kV.

1.3.2.2 Molecular weight

The molecular weight of a polymer influences the viscosity of the solution and has an important effect on the fiber morphology. Decreasing the molecular weight of poly(vinyl alcohol) while maintaining other parameters constant resulted in beads. Higher molecular weight poly(vinyl alcohol) resulted in smooth fibers initially followed by a ribbon like fibers [22]. In case of polyacrylamide (molecular weight 9 X 10^6 g/mol), even at a very low concentration solution exhibited a defect in fiber morphology. The concentration of such polymers should be varied between 0.3 to 3.0 wt % and beyond the suggested range results in a significant change in surface tension, viscosity and surface morphology [22]. A study on the melts of polypropylene with varying molecular weights showed an increase in the fiber diameter with molecular weight. High molecular weight polymers show the highest degree of entanglement and poses difficulties for the electric field to pull on individual polymer chain to obtain a thin fiber [23].

1.3.2.3 Solution viscosity

Viscosity determines the solution's ability to form fibers. Smooth continuous fibers can be obtained at optimum viscosity for a particular polymer solvent combination. The viscosity, molecular weight of the polymer and polymer concentration are interrelated and one cannot be independently judged. Low viscosity fails to form the fibers, while high viscosity requires higher electric field for electrospinning making it hard to operate [21, 24]. Baumgarten observed the formation of fine droplets at lower viscosity and incomplete

drying. At higher viscosity the droplets bumped into each other in the mid-air due to incomplete drying with acrylic polymer [25]. When a solution has low viscosity, surface tension dominates the process of fiber formation, but at optimum concentration it's the combined effect of both parameters [22, 26-29]. Yang et al. suggested a mixed solvent system of dimethylformamide and ethanol (50:50) for obtaining the best electrospun fibers of poly(vinyl pyrrolidone) and attributed the success to the combined effect of solution viscosity and charge density [10].

1.3.2.4 Surface tension of the solution

Surface tension is the measure of cohesive forces between the molecules in solution form and is dependent on the solution composition, polymer and solvent(s) used. Yang et al. studied the influence of solvents on the formation of nanofibers with poly(vinyl pyrrolidone) and concluded that lower surface tension with high viscosity formed smooth nanofibers with ethanol as solvent. They proposed the use of a multi-solvent system to obtain optimum surface tension and viscosity parameters for better electrospun fibers [10]. Like viscosity, surface tension can define the range of solvents and concentrations to be used in the electrospinning process [18].

1.3.2.5 Conductivity and surface charge density

The impact of conductivity and surface charge density of solution might not be as significant as other factors; nevertheless, it is important to have high conductivity for a greater charge carrying capacity. A highly conductive solution experiences a stronger

tensile force in an electric field compared to the less conductive solution making the former preferable for electrospinning. For preparation of acrylic microfibers, Baumgarten reported that the jet radius is dependent on the inverse cube root of electric conductivity [25]. Natural polymers being polyelectrolytic have better charge carrying ability and leads to poor fiber formation compared to synthetic polymers [30]. Hayati et al. observed that stable jets could be obtained by semi conducting liquids by applying sufficient voltage. Due to insufficient free charges, the insulating liquids like paraffin oil could not build electrostatic charge on the surface, while highly conducting water produced unstable stream and sparking at higher electric fields. So, insulating liquids and semiconducting liquids could produce stable fibers [31]. Yet another study on poly(vinyl alcohol) solution showed that the addition of a little amount of sodium chloride drastically increased the conductivity and decreased the fiber diameter [17]. Addition of sodium chloride has an effect in decreasing the occurrence of beads in PEO solution [32]. In addition, sodium phosphate [30], potassium phosphate [30], ammonium chloride [32], lithium chloride [32], are also used to obtain better fibers by changing the conductivity of solutions. Huang et al. used compounds soluble in organic solvents like pyridine that reacts with formic acid in solution to form a salt. Pyridine improves the conductivity and can be easily removed to obtain dry fibers. The addition of 0.4% wt of pyridine doubled the electrical conductivity of 2% nylon-4,6 in formic acid [33].

1.3.2.6 Solvent Volatility

The distance between the tip of the capillary and the collector is only a few centimeters long and the path taken by the jet to reach the collector is a few folds more. The fibers formed during the process are porous and dry fast depending on the choice of the solvent

used for solubilization of the polymer. The insufficiently dried fiber may attach to itself mid-air [25], form ribbon like fibers [19] or attach to itself after depositing on the collector. A study on polystyrene fibers showed that the use of more volatile tetrahydrofuran (THF) as a solvent produced high density pores and increased the surface area of fibers by up to 40%. The same polymer in DMF lost the microtexture completely. A combination of these solvents in different ratios gave different morphology profiles as the volatility of the mixture varied [19].

1.3.3 Types of electrospinning

The type of electrospinning process can have a significant impact on the fiber formation in addition to the process and solution parameters. Two main aspects to deal with in the type of electrospinning are nozzle configuration and solution vs melt electrospinning [6].

1.3.3.1 Nozzle configuration

Nozzle configuration is the number and the arrangement of capillary tubes from which the jets of fibers emerge. A single nozzle configuration is the simplest and the most common configuration where the charged solution flows through single capillary (Figure 1.1). This process has been used to electrospin different polymeric fibers either singly [34, 35] or in combination [36] or solvent systems [10]. Co-electrospinning of polymer blends in the same solvent or a mixture was the first and most common modification in the process. Zhou et al. mixed polyaniline with poly(ethylene oxide) in chloroform to obtain the nanofibers of size below 30 nm [37]. Sometimes polymer blends are to be used to obtain the final properties of fibers. If the polymers are not miscible in a common solvent or when

a homogeneous solution of polymers cannot be obtained, thermodynamic and kinetic aspects should be considered for electrospinning. One way out of that problem is to modify the nozzle configuration where different polymer solutions are electrospun from different capillaries side-by-side. In this type of configuration, two polymer solutions pass through separate capillaries arranged side-by-side, which are connected to a high voltage supply and never come in contact till they reach the end of the capillary. A single Taylor cone is formed which ejects the jet with non-uniform mixture of both the polymer solutions and after drying is deposited in the collector (Figure 1.3). For this type of configuration to work it is necessary that both the polymeric solutions have similar conductivity for them to form a single Taylor cone and eject as a mixture. A two bicomponent system consisting of poly(vinyl chloride)/segmented polyurethane and poly(vinyl chloride)/poly(vinyl fluoride) was studied [38].

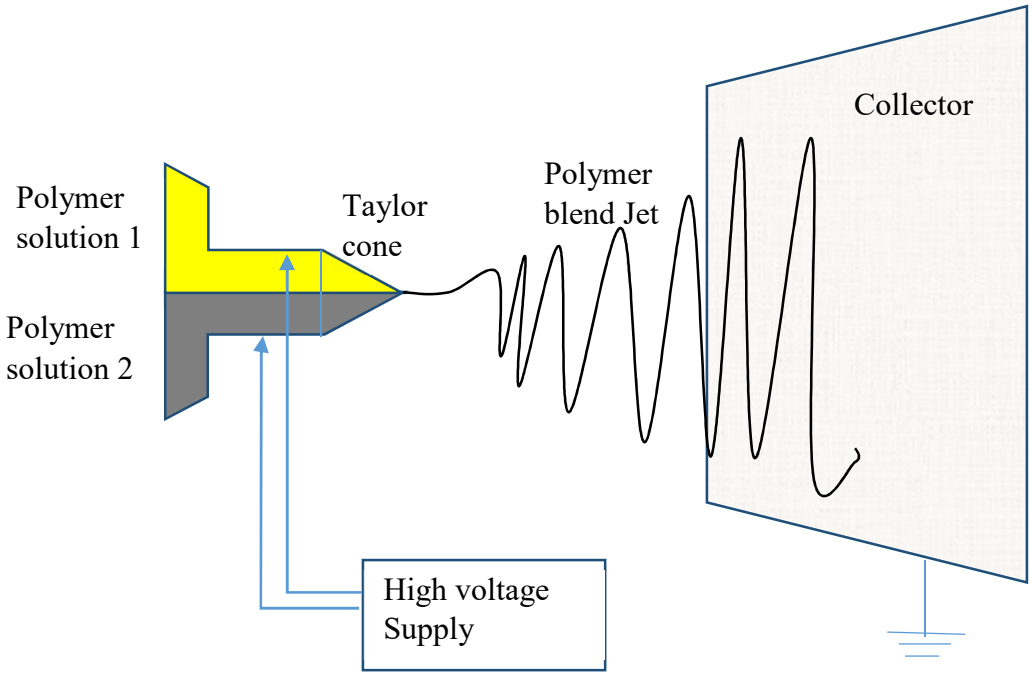

Figure 1.3: Side-by-side electrospinning schematic diagram: Polymer solutions 1 and 2 pass through separate capillaries which are connected to the high voltage supply. A single Taylor cone is formed which ejects the jet with non-uniform mixture of both the polymer solution and after drying is deposited in the collector.

A second type of nozzle configuration has recently been introduced is coaxial configuration. Two separate polymer solutions flow through two different capillaries where the small capillary is within the larger capillary. This configuration can easily encapsulate a small fiber within a larger fiber forming core-shell morphology (Figure 1. 4). In one study, living cells were encapsulated in poly(dimethylsiloxane) fiber with high cell viability (67.6 ± 1.9%) compared to the control cells (70.6 ± 5.0%). Though the initial viability was comparable, over time issues with cell morphology and growth rate were observed. It's the first study of its kind and authors noted the need for further research to

obtain the best possible results for encapsulation of living cells [39]. Encapsulation of a model protein, fluorescein isothiocyanate conjugated bovine serum albumin, with poly(ethylene glycol) in poly (epsilon-caprolactone) was able to sustain the release of drug, defining its use in drug delivery. Apart from the regular parameters which affect the quality of fibers being produced by the coaxial electrospinning, the relative flow rate of the core and the shell solutions is important in determining the encapsulation efficiency [40]. This method is widely used for the in tissue engineering to achieve sustained, local and efficient gene and growth factor delivery to the cells [40-42]. Few researchers have also used this method for the delivery of pharmaceutical compounds [43-45]. Though this method is now widely used, it still has the drawbacks on complexity of design and precise control of spinning parameters like interfacial tension, viscoelasticity of the polymers or two different solutions used.

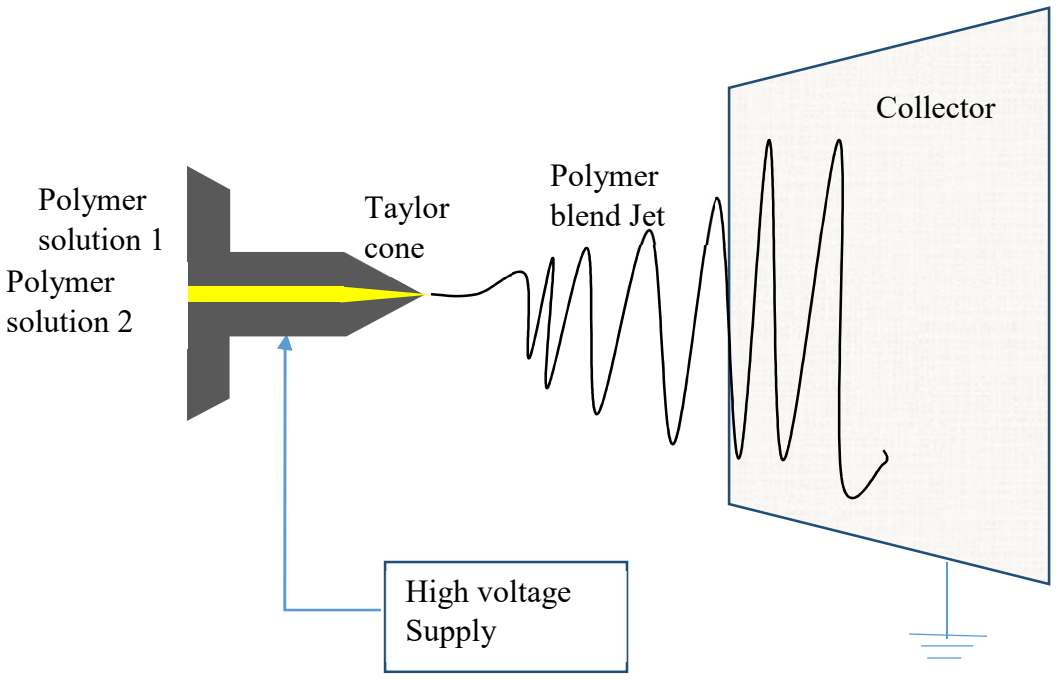

Figure 1.4: Coaxial electrospinning schematic diagram: Polymer solution 2 (yellow) is passed through the inner capillary tube while polymer solution 1 is passed through the outer capillary tube. The Taylor cone is formed where the inner solution (polymer solution 2) is surrounded by outer solution. The jet erupts from the Taylor cone and during that process the polymer in the inner layer is coated with the polymer in the outer layer. The dried fiber with core-shell is deposited in the collector.

The multi-jet electrospinning based on multiple capillaries arranged in circular geometry is yet another modification of nozzle that can both increase the throughput and facilitate scale up and commercialization. This modification increases the mat thicknesss, deposits

in the larger area and can mix fibers of different materials for better strength and versatility of use [46, 47]. In the study by Varesano et al., the morphology of PEO fibers was found to be acceptable in both polarities applied in standard and reverse configuration [47]. The main drawback of multi-capillary method is the alteration of electric field due to the presence of other electrospinning jets in the vicinity [48]. This can be overcome by using an auxiliary electrode of any polarity [49] or by using secondary electrode [50]. Hong et al. fabricated elastic, fibrous, composite sheet with biodegradable poly(ester urethane) urea (PEUU) and poly(lactide-co-glycolide) (PLGA) using two-stream electrospinning setup with rotating metal rod as the collector [51]. Such composite sheets possessed better breaking strains, tensile strength and suture retention capacity. In a review article, Persano et al. discussed different multi-jet configurations and the further possibilities of syringe-free approaches to multi-jet electrospinning [52].

1.3.3.2 Solution vs melt vs emulsion electrospinning

Electrospun fibers are generally obtained from polymer solutions or melts or emulsions. Melt spinning has high-throughput rate and process safety; solutions have the advantage of using a large variety of polymeric materials, lower energy consumption and superior mechanical, optical and electrical properties of prepared fibers. Emulsion electrospinning is significant for high melting polymers to prepare flame retardant fibers. A comparison of different spinning methods using poly(lactic acid) as a model polymer has been done by Gupta et al. [53].

The melt of the polymer with other additives is extruded through the capillary resulting in a thin fiber that gets rapidly cooled and solidified during its time in the air before depositing onto the collector [53]. Take-up speed, drawing temperature and draw ratio define the structural and tensile properties of the fiber. Draw ratio is the amount of stretching, which the material undergoes during drawing stage of electrospinning. The increase in draw ratio [54] and the take-up speed [55] increased the molecular chain orientation along the fiber axis and overall crystallinity of fibers formed from the melt. A higher entanglement of polymer amongst themselves gives sub-par fibers compared to the solution of the same polymer.

The solution spinning method is ideal for polymer or blend of polymers which are thermally unstable or degrade on melting. Based on how the solvent used for preparing the polymer solution is removed from the fibers, this method can be divided into two different types viz. dry spinning and wet spinning. The dry spinning process used hot air or inert gas on the polymer jet to facilitate the solvent evaporation and fiber solidification. For example, Postema et al. used a solvent combination of chloroform and toluene to produce PLA fibers of high strength by using dry spinning and hot-drawing process. They were able to obtain an optimal tensile strength of 2.2 GPa by electrospinning at 25°C [56]. Wet-spinning process involves the use of viscous coagulation bath containing the liquid which is miscible with the spinning solvent but not with the polymer. The interaction between the polymer solvent and non-solvent leads to phase separation and then solvent removal from the jet. This process is known to show fiber defects which can, to some extent, be limited by using

3-5 mm of air gap before the non-solvent as this allows for stress relaxation of the polymeric chain [53].

In the emulsion electrospinning process, finely ground polymers, insoluble and non-melting, are mixed with another polymer solution with a catalyst and emulsifying agents. The formed emulsion is then electrospun either by dry or wet spinning method. This technique has been used in preparing fibers from fluorocarbons with high melting point, ceramics, polymer blend with flame retardant properties [52]. Persano et al. have discussed in detail about the methods and their industrial application in their review paper [52].

1.3.3.3 Collector modification

The collector plate can be configured based on the application of polymeric fibers. Commercially, the most common ones include a stationary plate (or an aluminum foil) and a rotating plate. Both these types of collectors can further be subdivided into continual or patterned. Continual collector is simple and can be used to obtain fibers with a random internal structure on a stationary type, while some degree of directional control can be gained with higher speed in rotating collector. The patterned collectors have thin conductive wires separated from each other by an air gap. During the process, the fibers are deposited either between or perpendicular to the wires, individually, achieving some degree of alignment. Properly aligned polymer fibers are mostly useful in tissue engineering. In the rotating type of patterned collector, operation at lower speed deposits fibers between the conductive wires, while the deposits at the higher speed is dependent on electrostatic and mechanical forces increasing the degree of alignment. For research

purpose different designs of collector, mesh [57], pin [58], grids [59], liquid bath [60, 61], rotating rods [62], rotating cylinder [63], parallel bars [62], rotating drum with wire wound on it [64] and disc [27, 65] have been used.

1.3.3.4 Polarity inversion

The normal process of electrospinning is to apply a highly positive or negative charge to the solution/melt, which is to be electrospun and ground the collector. The reversal of polarity obtained by grounding the solution in capillary and charging the collects resulted in inconsistent findings. Kilic et al. studied the effect of polarity on the electrospinning process of 7.5 wt % poly(vinyl alcohol)/water solution on production efficiency and nanofiber morphology. They concluded that due to the lack of coulombic force acting on the polymer jet, the new reversed setup resulted in less nanofiber production. They also reported that the diameter and pore size of the web layer were much finer and homogeneously distributed in the conventional setup [66]. On the other hand, Varesano et al. reported the production of good quality nanofibers with mult-jet electrospinning using conventional and reverse polarity [47].

1.4 Methods of incorporating drugs

Electrospinning is easy, cost effective, offers great flexibility in selecting materials, high loading capacity and high encapsulation efficiency makes it suitable for many medical and drug related research. There are various methods of drug loading in the polymeric solution for electrospinning.

1.4.1 Blending

Blending is the primary method for incorporating drug into the polymer solution by dissolving or dispersing the drug and then subsequent electrospinning. Though this method is simple and easy the physicochemical properties of the drug and the polymer needs to be precisely considered as it affects the encapsulation efficiency, drug distribution in the fiber and the kinetics of the drug release. Lipophilic drugs (ie., paclitaxel) should be dissolved in lipophilic polymer and hydrophilic drug (ie., doxorubicin hydrochloride) in hydrophilic polymer for better encapsulation. When the drug is not dissolved properly in the polymer solution the dispersion is obtained which might lead to burst release if the drug migrates to the fiber surface [67]. To obtain a sustained release of the drug from the electrospun fibers, to enhance the drug loading efficiency and to reduce the burst release, different combinations of the mixtures of hydrophilic and hydrophobic polymers are used [68-70]. This process was modified by Ma et al. to obtain highly porous chitosan nanofibers by electrospinning chitosan/polyethylene oxide (PEO) blend solutions and then removing PEO with water [71]. They then soaked the porous nanofibers in 0.1 wt% paclitaxel solution to load the drug and then into 4 wt% hyaluronic acid for encapsulation. Mickova et al. in their research have compared electrospinning of liposome by blending and by coaxial electrospinning, and have reported that the blend electrospinning could not conserve intact nanofibers [72].

1.4.2 Surface modification

Surface modification is the technique where the therapeutic agent is bound or conjugated to the fiber surface to make them structurally and biochemically similar to the tissue. The drug release in this case will be attenuated and the functionality of the biomolecules will be protected [73]. The burst release and short term release will be mitigated with this strategy, making it highly applicable for slow and prolonged delivery of gene or growth factors. Incorporation of DNA, growth factors and enzymes in conjugation with fibers preserves their bioactivity and functionality [73-76]. The modulation of drug release can also be obtained if surface modification is done on a blended electrospun fibers. Im et al. fluorinated the electrospun fibers to obtain controlled release of the drug by introducing a hydrophobic group onto the surface [77]. In one modification, Yun et al. oxyfluorinated the multi-walled carbon nanotubes (MWCNTs) to introduce the functional groups and improve the compatibility with the PVA/PAA polymer solution before electrospinning the composite mixture [78]. Kim et al. surface modified the fiber and loaded with siRNA to obtain better results in gene silencing and wound healing [79].

Co-axial electrospinning encapsulates the biomolecules like DNA into the fiber in contrast to surface localization of DNA fibers with blending process. Luu et al. reported that the transfection efficiency of the electrospun DNA was significantly lower than Fugene 6, a commercially available transfection mediation agent [80]. To overcome the drawback, electrospinning method was changed to coaxial to get a polymer coating around the biomolecules which not only modified the release, but also protected the core against the direct exposure to the environment [40, 41, 81]. For additional benefits, the shell polymer can also be loaded with other bioactive molecules like non-viral gene-delivery vectors

for delivering the released DNA [41]. Mickova et al. have shown that co-axial electrospinning in superior to the blending method for electrospinning a liposome [72].

1.4.3 Emulsion

Another approach is the process of formation of emulsion for electrospinning, where the drug or the protein solutions is emulsified within a polymer solution. The later acts as an oil phase and spinning such emulsion gives a well distributed fiber for low molecular weight drug [82] and core-shell for high molecular weight drug [83-86]. The success of this process is mainly dependent on the ratio of aqueous solution to the polymer solution. This governs the distribution behavior of the molecule in fiber which in turn determines the release profile, structural stability and bioactivity of the encapsulated biomolecules [83]. As the drug and the polymers are dissolved in appropriate solvents, avoiding the need of a common solvent, various combinations of hydrophilic drugs and lipophilic polymer can be used. Unlike coaxial spinning, emulsion spinning might damage the macromolecules like pDNA due to shearing force and interfacial tension between two phases. Such instances can be avoided by preventing denaturation by condensation of pDNA [84, 85].

1.4.4 Multi-drug delivery

This is a recent approach in which multiple drugs with or without similar therapeutic effects are combined and electrospun with suitable polymer(s) [87, 88]. Wang et al. have used drug loaded polymeric nanoparticles for the core and drug loaded polymer for the sheath

to obtain a chain like structure with distinct release behavior, enabling a program or temporality release of multiple agents [87]. Xu et al. have developed hydrophilic model drug (bovine serum albumin) loaded chitosan microspheres and suspended them into the poly(l-lactic acid) (PLLA) solution with a hydrophobic model drug (benzoin) and polyvinylpyrrolidone (PVP) as a release tuner [88]. It is difficult to achieve independent release of the drugs in a multidrug system as both drugs are held by the carrier which provides same diffusion pathways and matrix-degradation rate [81]. Okuda et al. have developed a multilayered drug-loaded electrospun nanofiber mesh fabricated for time-programmed dual release by sequential electrospinning. The formulation has four layers: the top layer is the drug-loaded mesh, the barrier mesh (blank polymer), the second drug-loaded mesh and the last basement mesh. This system provided for the development of electrospun fibers with controlled drug release and time of release by optimizing the fiber size, thickness of each layer and the relative position of the layer. Though the authors have used two dyes as model drugs, this approach is significant for the biochemical modulation in chemotherapy with multiple-anti tumor drugs [89]. The graphical presentation of the same is shown in figure 1.5.

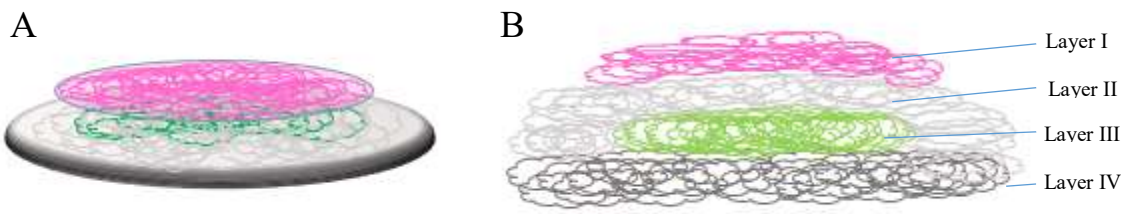

Figure 1.5: Graphical presentation of multi-drug delivery system, (A) overview, (B) cross sectional view, of a tetra layered sequential electrospun mesh. Cross-sectional view consists of drug loaded mesh (layer I), barrier mesh (layer II), second drug loaded mesh (layer III) and basement mesh (layer IV). Redrawn from [89].

1.4.5 Multilayer coated

Yet another innovative method of incorporation and delivery of drug combines the large suface area of electrospun fibers with polyelectrolyte multilayer structures [81]. Such multilayer uses either electrostatic or hydrogen bonding or acid-base pairing in layer-by-layer adsorption of polymers [90]. Chundar et al. have used two oppositely charged weak polyelectrolytes, polyacrylic acid (PAA) and allylamine hydrochloride (PAH), to produce nanofibers loaded with methylene blue as a model drug. In addition to polymers, a hydrophobic layer of perfluorosilane and PAA/poly(N-isopropylacrylamide) (PNIPAAM) were coated. The latter also provided temperature controlled drug-release properties. Im et al. used alginate and chitosan to coat the lactobacillus incorporated polyvinyl alcohol-based electrospun fibers. This formulation was designed to release lactobacillus in the large intestine after chitosan and alginate were dissolved in acidic and neutral environments of GIT [91].

1.5.Electrospun nanofibers in drug delivery

The electrospinning process has been used in drug delivery for treating various diseases. Electrospun fibers are mainly administered via oral and topical routes and as implantable systems. Table 1.1 provides a compilation of studies involving the use of electrospun fibers in drug delivery.

1.5.1 Transdermal delivery

Transdermal drug delivery system (TDDS) delivers the drugs locally or systemically via the skin. This is mainly suitable for the drugs which cannot be taken by the oral route either because of extensive degradation in the GIT or the drug undergoes extensive first pass metabolism [92]. Electrospun fibers for the transdermal application are mainly from the category of vitamins, anti-inflammatory and antioxidant drugs [78, 93-98]. Taepaiboon et al. have loaded vitamin A acid (all-trans retinoic acid) and vitamin E (α-tocopherol) in cellulose acetate polymer based electrospun fiber and solvent cast films [97]. The results obtained showed that the electrospun fiber mats showed a gradual and monotonous increase in the cumulative vitamin release in total immersion technique over the test period of 24 hours for vitamin E and 6 hours for vitamin-A loaded fiber. The corresponding solvent cast films showed a burst release of vitamins. A similar study performed by Nagwhirunpat et al. compared the electrospun and solvent cast film of polyvinyl alcohol loaded with meloxicam, an anti-arthritic drug [98]. They observed significantly higher skin permeation flux of the drug from electrospun fiber mats than the solvent cast film and the flux increased with increase in drug concentration in both the cases. Yun et al. developed an electro-responsive TDDS fibers by electrospinning poly(vinyl alcohol)/pol(acrylic acid)/multi-walled carbon nanotubes (PVA/PAA/MWCNT) with ketoprofen. The

swelling, drug release properties and conductivity of nanofibers were dependent on the MWCNT, oxyfluorination and oxygen content during oxyfluorination [78]. The fibers were found to be non-toxic and biocompatible with cell viability of more than 80%. In a similar study, Im et al. worked to understand the effect of MWCNT on the ketoprofen delivery in an electro-sensitive TDDS with polyethylene oxide and pentaerythritol triacrylate polymers [96]. This study supported the impact of MWCNT in influencing the conductivity and drug release behavior. Apart from the synthetic chemicals, natural/herbal extract containing asiaticoside from *Centella asiatica* has been incorporated into the electrospun fibers based on cellulose acetate polymer [93]. They used two forms of the drug, pure form of asiaticoside and crude extract from the plant for electrospinning. They observed better release profile from the pure drug than the extract in immersion method, while the release from both fiber mats were significantly low in pig skin method. In addition, they checked the release profile of the solvent cast films which were much lower. They further reported that the extract loaded fibers and films were toxic to normal human dermal fibroblasts at the extraction ratios of 5 and 10 mg/ml.

1.5.2 Antibiotics/antibacterial agents and wound dressing

Antibiotics and antibacterial agents are the most common drug molecules which are encapsulated in the recent times using different polymers and their combinations as carriers. Different polymers like PLA, PLGA and PCL are primarily used in the polymeric electrospun fibers for biodegradability and other natural and synesthetic hydrophilic or hydrophobic polymers are used to control the release pattern of the drug. Kenaway et al. used tetracycline hydrochloride with poly (ethylene-co-vinyl acetate) (PEVA), PLA and

their 50:50 blend to deliver the drug for treating periodontal disease [99]. They reported over 5 days of release with PEVA and the blend, suggesting their applicability in controlled release technology. Wang et al. have electrospun PVA nanofibers containing pleurocidin, a novel broad spectrum antimicrobial peptide, for the food preservations applications [100]. Direct application of the active moiety is not possible because of the loss in its bioactivity. This study reported higher inhibition efficacy of the drug from nanofibers against *Escherichia coli* in apple cider.

Wound dressings protect the wound from external microorganisms and absorbs/adsorbs the exudate from the wound providing the acceptable cosmetic appearance. The use of different components in the wound dresser prevents the infection of the wound and makes the healing process faster [101]. The components added to the inert dressings are mainly bioactives in the form of films, hydrogels, foams and sponges [70]. The wound healing with the electrospun fiber mats have the advantage of high surface area for efficient absorption of exudates, adjusts the moisture of wound, scar-free regeneration of skin cells and have porosity enough to supply oxygen for cell respiration, yet not enough for bacterial infections [101-103]. In one study by Jannesari et al., electrospun nanofibers of poly(vinyl alcohol) and poly(vinyl acetate) were prepared in individual and a 50:50 blend of the polymers. The nanofibers prepared using the polymer blend sustained the drug release and were found to be comfortable due to significant swelling [70]. In an *in vitro* microbial study, Said et al. have shown a faster bacterial colonization and biofilm formation in Fusidic acid loaded PLGA fibers; which in turn enhanced the release of drug and eradicated planktonic bacteria and suppressed biofilm [104]. Thakur et al. used the dual spinneret

electrospinning apparatus to prepare a single scaffold of lidocaine and mupirocin [105]. Two drugs with varying lipophilicities were found to have different release profiles. Lidocaine showed a burst release while mupirocin showed sustained release providing action for over 72 hours. Wang et al. have fabricated nanofibers of ethylene-co-vinyl alcohol (EVOH) with different antibacterial drugs and silver for wound dressing with superior germ killing capacity [106]. Silver nanoparticles have been used in many other studies for the similar applications [107, 108]. Recently, Chutipakdeevong et al. have utilized the hybridization method to combine the properties of *Bombyx mori* silk fibroin with poly(ε-caprolactone) (PCL) electrospun fibers [109]. The PCL fiber surfaces were coated with silk fibroin protein using lyophilization technique and then surface modified with fibronectin to improve their biological function. The surface modified hybrid showed significant proliferation of normal human dermal fibroblast (NHDF), followed by hybrid scaffold and then neat PCL fibers.

1.5.3 Delivery of anticancer agents

Anticancer agents like doxorubicin, paclitaxel, cisplatin and dichloroacetate have been incorporated into electrospun fibers with polymers like PLA, PLGA and PLLA for postoperative chemotherapy. Water-in-oil (w/o) emulsion, with water soluble drugs in aqueous phase and polymeric solutions of PEG-PLA in chloroform as oily phase, was prepared and electrospun to obtain fibers [110]. In a continuation study, hydrophobic paclitaxel and hydrophilic doxorubicin were simultaneously loaded in the emulsion based electrospinning process for multi-drug delivery [111]. The cytotoxicity study against rat Glioma C6 cells showed higher inhibition and apoptosis in combination therapy compared

to the single drug system. *In vitro* cytotoxicity study on the same cells in another study showed a sustained release of platinum based cisplatin for more than 75 days without burst release and four times better cytotoxicity than the free drug [112]. Lee et al. have fabricated biodegradable PLGA fibers sheets for local delivery of epigallocatechin-3-O-gallate (EGCG) to reduce intimal hyperplasia in injured abdominal aorta [113]. The EGCG loaded sheets exhibited initial burst release for 24 hours, followed by sustained release for more than 30 days in phosphate buffer. *In vivo* studies showed promising results against intimal hyperplasia after application of the EGCG loaded fibers compared to PLGA control.

Recently, electrospun fibers have been used for the local chemotherapy. Liu et al. encapsulated doxorubicin in PLLA polymer fiber and examined its efficacy for local chemotherapy against secondary hepatic carcinoma by wrapping the whole liver with carcinoma with the fiber-mat [114]. In the first 24 hours, the drug was rapidly released from the fiber to localize in the liver tissue. It also significantly inhibited the growth of tumor and increased the median survival time of the mice in the experiment. Luo et al. prepared fibers with core-loaded hydroxycamptothecin (HCPT) and 2-hydroxypropyl-β-cyclodextrin complexed HCPT and observed that the inclusion complex showed superior antitumor activity and fewer side effects compared to the free drug [115]. Ma et al. loaded paclitaxel in the porous chitosan nanofiber and then encapsulated the fiber by polyanionic macromolecular hyaluronic acid (HA). The MTT assay in prostate cancer cells showed that the drug loaded nanofiber mats were good in prohibiting cell attachment and proliferation [71]. The drawback of the fibers was an initial burst release of drug within first 48 hours. Chen et al. incorporated titanocene dichloride in PLLA polymer based fibers [116]. The

MTT assay in human lung tumor (SPCA-1) cells showed that drug content of 40, 80, 160 and 240 mg/L had the cell growth inhibition rates of 11.2%, 22.1%, 44.2% and 68.2%, respectively. Apart from the synthetic anticancer drug, natural products with anticancer properties and minimal side effects have been studied. Suwantong et al. electrospun curcumin in cellulose acetate solution and observed that curcumin is almost completely (~90 to ~95%) released in total immersion method, while considerably low values were obtained for transdermal diffusion through pig skin [95]. In another study, Shao et al. fabricated green tea polyphenols (GTP) in poly(ε-caprolactone)/multi-walled carbon nanotubes (PCL/MWCNTs) composite nanofibers by electrospinning. The cytotoxicity experiment showed a significant inhibitory effect in A549 and Hep G2 tumor cells [117].

1.5.4 DNA, RNA, Protein and growth factor delivery

The most commonly loaded bioactive materials in electrospun fibers include DNA, RNA, proteins and growth factors. The electrospinning process applied to the bioactive materials should be designed in such a way that the activity and functional efficacy of the material is preserved during and after electrospinning. Before coaxial electrospinning, few studies on bioactive materials have been done with blending process. The stability of the growth factors is the limiting aspect in formulating them in tissue engineered scaffolds. Human nerve growth factor (hNGF) was encapsulated with BSA as carrier protein into the nanofibers of PCL and poly(ethyl ethylene phosphate) (PCLEEP). The protein released in a sustained manner for more than 3 months from the electrospun fibers and showed partial retention of bioactivity [118]. The same group also co-encapsulated small-interfering RNA (siRNA) and transfection reagent (TKO) complexes within nanofiber of caprolactone and

ethyl ethylene phosphate (PCLEEP, diameter ~400 nm) to obtain a sustained release of siRNA for up to 28 days [119]. The release of siRNA was enhanced and more significant gene knockdown was obtained when compared with electrospun fibers of PCL containing siRNA [120]. Schneider et al. demonstrated that biofunctionalized silk mats containing epidermal growth factor (EGF) are extremely promising in achieving bioactive wound dressings for would healing process [121]. Similarly, Zhang et al. showed that the poly(ethylene carbonate-ε-caprolactone) scaffolds with VEGF maintained good growth and spread morphology in human umbilical vein endothelial cells [122]. After the introduction of coaxial electrospinning method, most biomolecules are preferentially encapsulated using this method forming a core of biomolecule and shell of polymer in core-shell structure. The polymeric shell protected and released biomolecules in a sustained manner. Saraf et al. prepared fiber scaffolds with plasmid DNA (pDNA) within the core of poly(ethylene glycol) and non-viral gene delivery vector poly(ethylenimine)-hyaluronic acid (PEI-HA) within the sheath polymer poly(ε-caprolactone) (PCL) by coaxial electrospinning [41]. They achieved a variable transfection activity over extended periods of time upon the release of pDNA and non-viral gene delivery vectors from electrospun fiber scaffolds. Mickova et al. have proposed the use of liposomes in the core of polyvinyl alcohol (PVA) and shell of PCL for protecting the enzymatic activity of horseradish peroxidase [72]. The encapsulated enzyme retained its activity because of the shielding effect of the lipid sphere of liposome. Chen et al. encapsulated chitosan/siRNA nanoparticles in PLGA by electrospinning to control the release behavior at different pH conditions. In addition, the encapsulated siRNA showed up to 50% enhanced green fluorescent protein (EGFP) gene silencing activity after 48 hours of transfection in H1299

cells [123]. Surface functionalization of nanofibers was performed for MMP-2-siRNA (Matrix metalloproteinase) in linear polyethyleneimine (LPEI) coated nanofibers with various nitrogen/phosphate (N/P) ratios [79]. In an animal study for 7 days, it was observed that the siRNA in these fibers increased the MMP-2 gene silencing effect and neo-collagen accumulation at the wound site. Fabrication of surface modified electrospun fibers containing growth factors conjugated with heparin or polysaccharides are getting common [73, 75, 124]. Burst release of nerve growth factor was observed from electrospun scaffolds conjugated with chitosan/poly(vinyl alcohol) [75]. Basic fibroblast growth factor was incorporated in heparin containing polyelectrolyte nanoparticle and that was electrostatically adsorbed on chitosan matrix to overcome the problem of burst release [73]. Han et al. fabricated a composite design containing poly(ethylene glycol)-poly-(ε-caprolactone) diacrylate (PEGPCL) hydrogels coupled with electrospun mats of poly(ε-caprolactone) to control the burst release and extend the release duration of nerve growth factor [125]. The bioactivity of the growth factor was demonstrated by PC-12 cells neurite extension. Further, immobilization and delivery of the growth factor for the bone tissue engineering is disused in the review by Chen et al.[126].

In addition, electrospinning has extensively been used and reviewed for tissue scaffold engineering with or without any active moiety incorporated in the polymeric matrix.

Table 1.1: Studies involving the use of electrospun fibers in drug delivery (partial listing).

Polymer(s)	Drug(s)	Solvent composition	Spraying type
Antibiotics/ Antibacterial agents			
PLA, PEV, PLA/PEVA	Tetracycline hydrochloride [99]	Chloroform	Single nozzle
PLA/PCL	Tetracycline hydrochloride [127]	Chloroform, dimethylformamide	Single nozzle
PLLA	Tetracycline hydrochloride [43, 45]	Chloroform: acetone (2:1)	Coaxial
PCL	Gentamycin sulfate and Resveratrol (antioxidant) [44]	Chloroform: ethanol (3:1)	Coaxial
PVA, Poly(vinyl acetate)	Ciprofloxacin Hydrochloride [70]	Diluted acetic acid solution	Single nozzle
PLGA	Fusidic acid and rifampicin[128]	Tetrahydro Furan/Dimethylformamide	Single nozzle
PEUU and PLGA	Tetracycline hydrochloride [51]	1,1,1,3,3,3-Hexafluoro-2-propanol	Single nozzle
PLGA	Mefoxin [69]	DMF	Single nozzle
PCL	Metronidazole benzoate [129]	Dichloromethane (DCM:DMF)	Single nozzle
coPLA, coPLA/PEG	Ciprofloxacin hydrochloride, Levofloxacin hemihydrate, Moxifloxacin hydrochloride [130]	DCM:DMSO (3:1)	Single nozzle
PLLA	Lidocaine and mupirocin [105]	Hexafluoroisopropanol	Dual spinneret
PCL	Ornidazole (Biteral®)	Chloroform and DMF (3:7)	Single nozzle
Chitosan/PEO	Potassium 5-nitro-8-quinolinolate [131]	2% (w/v) acetic acid	Single nozzle
PU	Itraconazole and ketanserin [132]	DMF, DMAc	Single nozzle
PVA	Pleurocidin [100]	Distilled water	Sinfle nozzle
NSAIDS and analgesics			
EC and PVP	Ketoprofen [133]	Ethanol-water	Single nozzle
PVA/PAA/MWCNT [78] PEO/PETA/MWCNT [96]	Ketoprofen	Deionized water	Single nozzle
PLGA PEG-g-CHN	Ibuprofen [134]	DMF	Side-by-side

PVP/Zein	Ketoprofen [135]	Ethanol-water	Coaxial
PLGA/Gelatin	Fenbufen [68]	2, 2, 2-trifluoroethanol	Single nozzle
Chitosan nanoparticles/PCL composite	Rhodamine B/Naproxen [87]	Acetic acid/chloroform:methanol (3:1)	Single nozzle yet core/sheath fiber
PVA	Meloxicam [98]	Water	Single nozzle
Proteins, DNA, RNA and human factors			
PEI-HA	plasmid DNA (pDNA) [41]		Coaxial
PCL	siRNA[120]	2,2,2-Trifluoroethanol (TFE)	Single nozzle
PCL-co-PCLEEP	Human glial cell-derived neurotrophic factor [136]	Dichloromethane	Single nozzle
PCL-co-PCLEEP	Human β-nerve growth factor [118]	Dichloromethane	Single nozzle
PECCL	Endothelial growth factor VEGF [122]	-	Single nozzle
PCLEEP	siRNA [119]	RNase-free water	Single nozzle
Chitosan/PLGA	siRNA [123]	Hexafluoro-2-isopropanol/water	Single nozzle
PEO	Bovine Serum Albumin (BSA) [137]	Deionized water	Single nozzle
PLA	Lysozyme [83]	Chloroform	Emulsion
Poly(L-lactide-co-caprolactone)	Human-nerve growth factor (NGF) [138]	Chloroform	Emulsion
PLA-PEG and PLGA	DNA [80]	DMF	Single nozzle
Poly(urethane)	Growth factors (VEGF, PDGF) [42]	Chloroform: ethanol (75:25)	Coaxial
PVA/PCL	Horseradish peroxidase [72]	-	Coaxial
Anticancer agents			
PEG-PLA	Doxorubicin Hydrochloride [139]	Chloroform	Single nozzle
PEG-PLA	Doxorubicin Hydrochloride [110]	w/o emulsion	Emulsion
PLLA	Doxorubicin [114]	Chloroform-methano-DMSO	Single nozzle

HPCD	Hydroxycamptothecin [115]	DMSO	Emulsion
PLGA	Paclitaxel [140, 141]	DCM and DMF	Single nozzle
PLA/PLGA	Cisplatin [112]	DCM	Single nozzle
PLA	Dichloroacetate [142]	Chloroform	Single nozzle
PEO and PEG-PLLA	1,3-Bis(2-chloroethyl)-1-nitrosourea [143]	Chloroform	Single nozzle/Emulsion
Chitosan/PEO/HA	Paclitaxel [71]	Acetic acid/distilled water	Single nozzle
Cellulose acetate	Curcumin [95]	Acetone/dimethylacetamide (2:1)	Single nozzle
PCL/MWCNT	Green tea polyphenols (GTP) [117]	Dichloromethane	Single nozzle
PLLA	Titanocene dichloride [116]	Dichloromethane	Single nozzle
Tissue Engineering			
Collagen-PEO	Wound healing, tissue engineering, hemostatic agent [144, 145]	Hydrochloric acid	Single nozzle
Poly(ε-caprolactone)	Adenovirus with gene for green fluorescent protein [40]	Chloroform: ethanol (75:25)	Coaxial
PDLLA/PLGA	Guided tissue regeneration [146]	Chloroform:DMF (9:1) and THF/DMF (3:1)	Single nozzle

PLA: Poly(lactic acid); PEVA-Poly(ethylene-co-vinylacetate); PCL: poly(ε-caprolactone); PCL-co-PCLEEP: Copolymer of caprolactone and ethyl ethylene phosphate; PLGA: Poly(D,L-Lactic acid-co-glycolic acid); PEUU: poly(ester urethane) urea; EC: ethyl cellulose; PEO: Poly(ethylene oxide); PU: Polyurethane; DMAc: Dimethylacetamide; PETA: pentaerythritol triacrylate;]PEI-HA: Poly(ethylenimine)-hyaluronic acid; PVP: polyvinylpyrrolidone; PEG-g-CHN: poly(ethylene glycol)-g-Chitosan; PEG-PLA: poly(ethylene glycol)-poly(lactic acid); PLLA: poly(L-lactic acid); HPCD: 2-hydroxypropyl-β-cyclodextrin; HA: Hyaluronic acid; MWCNT : multi-walled carbon nanotubes, PAA – Poly(acrylic acid); PECCL: poly(ethylene carbonate-ε-caprolactone); MWCNT-Multi-walled carbon nanotube; PDLLA: poly(D, L-lactic acid)

1.6 Conclusions

Electrospinning process has generated a lot of interest in various medical applications due to its ease of use, adaptability and flexibility in controlling the fiber diameter from micrometer to the nanometer range. Though this method has been in use for a few decades now, the technique and the equipment used in the electrospinning process are ever-evolving. Electrospinning started its journey with a single nozzle configuration and later evolved into multi-nozzle configurations through coaxial and emulsion spinning configurations. Further studies are being carried out to modify the nozzle configuration and collector design in order to significantly improve fiber properties and simplify the manufacturing process. This review summarizes a few aspects of electrospinning with a special emphasis on the use of electrospun fibers in drug delivery. By careful selection of polymers, it is now possible to deliver various antibacterial agents and anticancer drugs in a required manner using electrospun nanofibers. In order to make further progress, particularly in the field drug delivery, it is necessary to identify ways that allow large-scale fabrication of nanofibers with desired morphological and mechanical properties in a reproducible manner. Despite relentless efforts being made by academic and industrial scientists, much of research conducted with electrospun fibers is *in vitro*. Further progress in the field of electrospun nanofibers will require the continued assessment *in vivo.* Scientists working in this field have to identify ways to use nanofibers for immunotherapy and gene therapy in order to meet the future demands in drug delivery.

Chapter 2

Significance of research

Drug delivery to the eye still remains a challenge due to the intricate physiological and anatomical structure of the eye. The anatomical position of the eye allows local delivery of drugs along with non-invasive clinical assessment of disease, while the physiological barriers prevent the entry of drug substances. For efficient treatment of diseases, drug molecules should circumvent the protective physiological barriers without causing permanent tissue damage. Both anterior and posterior segments provide unique barriers to the entry of drugs [147, 148]. These barriers vary based on the route of administration such as topical, systemic and injectable. For instance, topical administration results in very low ocular bioavailability (<5%) due to various barriers such as non-productive absorption, tear production, tear turnover, solution drainage, transient residence time, and impermeable corneal epithelium. Anterior segment ocular diseases are primarily treated using conventional ophthalmic dosage forms such as eye drops, suspensions and ointments [149].

Dexamethasone has a potent anti-inflammatory activity with an optimum log P value that allows permeation into the lipophilic corneal epithelium. Dexamethasone is widely used in treating anterior segment inflammations. Dexamethasone is marketed as an eye drop suspension due to its limited water solubility. The drug release and absorption from a

suspension dosage form, especially meant for the eyes, is highly unpredictable. Similar formulations with the identical concentrations of active and inactive ingredients tend to exhibit differences due to varying physicochemical properties [150]. Moreover, proper topical administration of drugs could be challenging for many elderly patients and effective delivery systems that bypass the patient adherence factor and reduce side effects have the potential to fundamentally improve patient care and clinical outcomes. The inherent disadvantages of suspension dosage forms have encouraged researchers to look for alternate strategies to deliver dexamethasone.

An ocular insert is a thin, multilayered, polymeric device capable of delivering drugs at a constant rate. Ocular inserts minimize the side effects by limiting systemic exposure and increasing the contact time of the drug with ocular tissues. Despite a few disadvantages, biodegradable ocular inserts could be manipulated to achieve a safe and effective therapy. This study presents the "proof-of-concept" data to show that electrospun inserts perform better than inserts prepared by solvent casting technique and are capable of delivering drugs in a sustained fashion. The purpose of this work was to develop, characterize and compare electrospun and solvent cast polymeric inserts for ocular drug delivery. Poly (lactic acid) (PLA) is a biodegradable polymer approved by the FDA for use in biomedical applications. However, its hydrophobicity is a major drawback to its use in fabricating an ocular insert. Thus, a blend of PLA with poly (vinyl alcohol) (PVA), which is hydrophilic and water soluble, is used in the preparation of inserts for obtaining flexibility, surface hydrophilicity, and the required drug-release rate from inserts.

There are only a few patented ocular inserts with commercial value [151], and this product has the potential to be marketed. To our knowledge, this is the first application of electrospinning for the ocular drug delivery of dexamethasone for treating anterior segment inflammatory diseases.

Chapter 3

Comparison of electrospun and solvent cast PLA/PVA inserts as potential ocular drug delivery vehicles

3.1 Abstract

Purpose: The purpose of this work was to develop, characterize and compare electrospun nanofiber inserts (ENI) and solvent cast polymeric inserts for ocular drug delivery. **Methods:** ENI and solvent cast inserts (SCIs) of dexamethasone were fabricated using a blend of poly-lactic acid (PLA) and poly-vinyl alcohol (PVA). Inserts contained 1%, 5% and 10% dexamethasone (by weight). Inserts were characterized for morphology, thickness, pH in simulated tear fluid (STF, pH 7.4), drug content, thermal characterization, infrared (IR) spectroscopy, *in vitro* drug release, dimethylformamide (DMF) and chloroform content and cytotoxicity in cultured bovine corneal endothelial cells. The inserts were sterilized by UV radiation for 10 minutes and tested for sterility using plate and direct inoculation.

Results: The thickness of 1%, 5%, and 10% dexamethasone-loaded ENIs were found to be 50 μm, 62.5 μm, and 93.3 μm, respectively with good folding endurance. Inserts prepared using the solvent casting technique were brittle with thickness values greater than 200 μm. The release rate of dexamethasone from 1%, 5% and 10% ENIs were found to be 0.62 μg/h, 1.46 μg/h, and 2.30 μg/h respectively, while those from solvent casting technique were erratic. A sustained release of dexamethasone was observed from 10% inserts for up to 36 hours. The quantities of DMF in ENIs and SCIs were found to be

0.007% w/w and 0.123% w/w, respectively. The chloroform content in both the inserts was below the detection limit. In addition, the inserts were sterilized by UV radiation and tested for sterility by direct inoculation in tubes and plate inoculation method in a petri dish. No cytotoxicity was observed from ENIs in cultured bovine corneal endothelial cells for up to 24 hours.

Conclusion: Based on the results obtained, we conclude that ENIs are better than inserts obtained by solvent casting technique and could be utilized as a potential delivery system for treating anterior segment ocular diseases.

3.2 Introduction

The anterior segment of the eye includes tissues such as the cornea, iris, ciliary body conjunctiva and lens [152]. The anatomical position of the eye allows topical application of drugs for treating the anterior segment eye diseases. However, the entry of the drug into the eye is hindered by physiological barriers such as blinking, induced lacrimation, tear turnover, nasolacrimal drainage and the cornea [153]. The cornea is comprised of five layers: the outermost corneal epithelium, the Bowman's layer, the corneal stroma, the Descemet's membrane and the inner corneal endothelium. The corneal epithelium acts as a barrier against hydrophilic drugs, while the stromal layer is a barrier for hydrophobic drugs [154, 155]. So, the drug molecules with an optimal logP value of 2-3 are considered suitable for crossing the corneal barrier [156]. Conventional dosage forms like eye drops, suspensions and ointments are topically applied to treat most anterior segment diseases. Approximately, 90% of the marketed ophthalmic formulations are conventional dosage forms of which two-thirds are solutions, while the rest are ointments and suspensions [149, 157]. Novel dosage forms like liposomes [158], nanoparticles [159] and implants [160] have also been researched for ocular delivery.

Dexamethasone is a yellowish-white, odorless, crystalline synthetic anti-inflammatory adrenal corticosteroid with limited aqueous solubility (~1 mg/10 ml) [161] and moderate lipophilic nature with log P value of 1.83 [162]. Dexamethasone works by entering the cells and blocking the production of vascular endothelial growth factor and prostaglandins, substances that are responsible for inflammation and swelling at the injured sites [163-166]. Ophthalmic formulations of dexamethasone are used in treating steroid-responsive

inflammatory conditions like allergic conjunctivitis, acne rosacea, superficial punctate keratitis, herpes zoster keratitis, iritis, cyclitis and corneal injuries from chemical radiation, thermal burn, or penetration of foreign bodies. Additionally, dexamethasone is also indicated for posterior segment diseases such as macular edema following branch retinal vein occlusion (BRVO) or central retinal vein occlusion (CRVO), non-infective posterior uveitis and diabetic macular edema [167, 168]. For treating anterior segment inflammations, the usual dose of dexamethasone ophthalmic suspension drop, Maxidex®, is one drop in the affected eye(s) every 4 hours. However, in severe inflammations the dose could be increased to 1-2 drops every 30-60 minutes until a reasonable response is obtained or alternative therapy is indicated [168]. Similarly, Maxidex® eye ointment (Alcon Laboratories, Fort Worth, TX) is applied up to four times daily into the conjunctival sac. Both these formulations are applied for a few days to weeks depending on the disease and severity [169]. The suspension eye drop is supplied in a plastic "droptainer" for self-administration and this poses problems for children and even adults, as drug content shows high degree of variation due to patient's inability to either squeeze or aim adequately [170]. The drug release and ocular absorption from a suspension is highly unpredictable and due to the difference in physiochemical properties, even identical formulations tend to vary from each other in their release profile [150]. It has been reported that the continuous application of the dexamethasone eye drops (0.1%) could cause thinning of cornea/sclera, defects in visual acuity, posterior subcapsular cataract and even glaucoma accompanied by optic nerve damage [171]. Ophthalmic ointment of dexamethasone, which has now been discontinued in the US, also suffers from the problem of content uniformity during application and blurred vision [172]. In addition, the natural barrier and protective

mechanisms of the eye are responsible for precorneal drug loss and low bioavailability of less than 5% [173]. The usual tendency to compensate for the low ocular bioavailability is to either increase the concentration of drug or dosing frequency, both of which significantly increase the chances of local and systemic toxicity [173-175] and more erratic and unpredictable drug delivery. Several alternative delivery strategies of dexamethasone such as gels [176], nanoparticles [171], microemulsions [177], nanomicelles [178-180], injections [181], soluble ophthalmic inserts [182] were reported in literature for enhancing the ocular retention and bioavailability of the drug. Ozurdex® is an intravitreal implant of dexamethasone which has been approved for treatment of macular edema, posterior uveitis and diabetic macular edema

The ophthalmic inserts are the dosage form of choice as they increase the contact time and sustain the duration of release [183]. In addition, they provide more accurate dosing, reduce systemic absorption, and reduce frequency of administration, thus improving the patient adherence. There are different methods of preparation of inserts viz. solvent casting [184, 185], film casting [186, 187], tableting [188] and molding/extrusion [189]. Electrospun fiber mats have extensively been used in tissue culture, drug delivery [6, 190] and wound dressing [190]; however, the use of electrospun fibers as ophthalmic inserts is relatively unknown. To the best of our knowledge, no studies are reported in the literature describing the application of electrospun inserts for ophthalmic drug delivery. Electrospinning is a process of forming micrometer to nanometer sized polymeric fibers, either hollow or solid, with the application of the electric force in the polymeric solution at the tip of a conducting tube. It is one of the most commonly used techniques to obtain continuous fibers in the nanometer size range [1-3]. Electrospun ocular inserts of biodegradable polylactic acid

(PLA) and polyvinyl alcohol (PVA) could be cost-effective and easy to manufacture on a large scale. We have previously used the electrospinning technique in tissue engineering and orthopedic applications **[**191-194**]**.

In this study, we have prepared ophthalmic inserts of dexamethasone containing 1%, 5% and 10% using electrospinning technique and compared them with those prepared by solvent casting technique. In the solvent casting technique, polymer(s) and drug(s) are dissolved in a low boiling point solvent. The mixture is poured onto a flat surface and the solvent is evaporated to obtain a thin fiber mat. The solvent casting technique was chosen for the comparison as it is the most extensively used technique in the preparation of ophthalmic inserts. Inserts were characterized for morphology, thickness, pH in simulated tear fluid (STF, pH 7.4), drug content, thermal characterization, *in vitro* drug release, dimethylformamide (DMF) and chloroform content, cytotoxicity and sterility.

3.3 Materials and Methods

3.3.1 Materials

Dexamethasone (Lot C137572) was procured from PCCA (Houston, TX). Polylactic acid was procured from Sigma-Aldrich. Polyvinyl Alcohol (Lot SLBM1859V) was procured from Sigma. Chloroform (Lot 114177), N,N-Dimethylformamide (DMF) (Lot 147977) were procured from Fisher Scientific. Sodium hydroxide (Lot YI0086) was procured from Spectrum Chemical (Gardena, CA). Potassium phosphate monobasic KH2PO4 (Lot 103497), polysorbate 80 (Lot 20589), tryptic soy broth (Soyabean Casein Digest medium-

Bacto™, Lot 2030828), DMSO (Lot 104549) and Mueller-Hinton agar (Lot 3240477) were procured from Fisher Scientific (Pittsburgh, PA). Phosphoric acid (Lot A0305025) was procured from ACROS (Fair Lawn, NJ). TACS® MTT reagent (Lot 31205J14) was supplied from Trevigen. RPMI Medium 1640 (Lot 1738144) was supplied from (Life technologies, NY). High Performance Liquid Chromatography (HPLC) solvents, including acetonitrile (Lot 121151) were purchased from Fisher Scientific (Pittsburgh, PA). Distilled deionized water used in the study.

3.3.2 Preparation of ophthalmic inserts

The polymeric inserts were prepared by two different methods: a) solvent casting technique and b) electrospinning technique. The solution for both procedures was prepared in a similar manner. Polylactic acid (PLA) and dexamethasone in varying concentrations of 1%, 5% and 10% were dissolved in chloroform. Three milliliters of dimethylformamide (DMF) was added to the beaker and the mixture was allowed to stand for 1 hour. Polyvinyl alcohol (PVA) was dissolved in deionized water at 90°C using a magnetic stirrer. PVA solution was slowly added to the beaker containing PLA, dexamethasone and DMF in chloroform solution under continuous mixing. The mixture was stirred to remove any air bubbles and to obtain a clear uniform solution. For solvent casting technique, the solution was poured into a glass petri dish (80 mm X 15 mm) with aluminum foil lining. The solution was then allowed to dry at room temperature. For slow, controlled and uniform evaporation of the solvents from the polymer solutions, a conical flask was inverted above the solution [195, 196]. For electrospun nanofiber inserts (ENIs), a setup containing a syringe pump, a DC voltage generator and an earthed metallic collector plate was used

(Figure 3.1). The working range for the pump rate was between 1.5 ml/h to 2.5ml /h; distance between the tip of the syringe and the collector plate was 8 -12 cm; applied voltage was between 10kV to 25 kV which were later optimized at 1.5 ml/h, 9 cm and 15 kV respectively. Figure 3.1 shows the schematic diagram of the setup and the process of electrospinning. The blank inserts for both methods were prepared in a similar manner without the drug. Inserts of containing about 50 µg of dexamethasone were cut, wrapped with aluminum foil and stored.

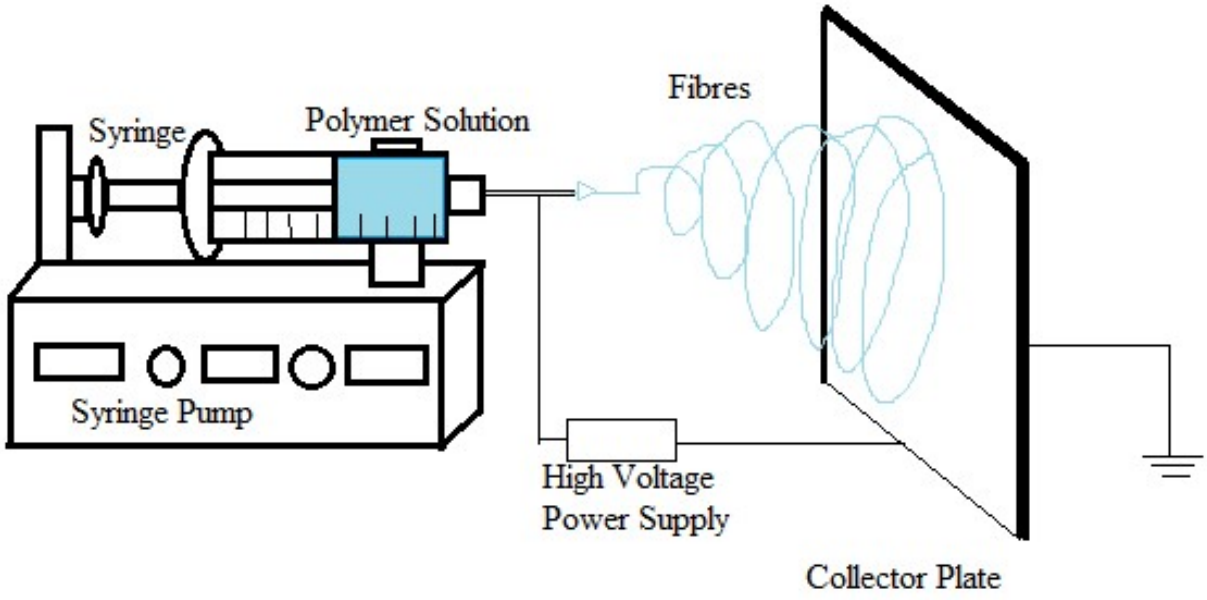

Figure 3-1: Schematic representation of electrospinning process.

3.3.3 HPLC Analysis of Dexamethasone

Waters HPLC (Alliance e2695 separation module, Milford, MA) with 2998 PDA detector and C8 reverse phase column (150mm X 4.6mm, 5µm particle size, Phenomenax column) was used for the analysis of dexamethasone. An isocratic mobile phase containing of

acetonitrile: water (50:50) was pumped at a flow rate of 1.0 ml/min. The injection volume was 10 µl and the absorbance for dexamethasone was measured at 242 nm. A stock solution of 1 mg/ml of dexamethasone was prepared in methanol. Calibration standards ranging from 0.39 - 50 µg/ml were prepared in the mobile phase. Each calibration standard was analyzed in triplicate, and the average peak area was plotted against the concentration.

3.3.4 Drug Content

For drug content analysis, a weighed quantity of inserts was placed in 2 ml of acetone in a closed glass vial and sonicated for 30 minutes. The acetone was then evaporated and 2 ml of methanol was added, mixed for 2 hours and centrifuged at 5000 rpm (Centrifuge 5430 R, Eppendorf) for 10 minutes. The supernatant was taken for analyzing drug content using HPLC. Drug content was measured in triplicate [197, 198].

3.3.5 Thickness measurement

The thickness of the inserts was measured using a digital micrometer (Mitutoyo Absolute Digital Caliper, Japan).

3.3.6 pH of solution

Inserts were placed into 2 ml simulated tear fluid (STF) of pH 7.4. The pH change of the fluids over the period of time was recorded using a calibrated Mettler Toledo SevenMulti™ pH/conductivity meter.

3.3.7 Wettability Study

Simulated tear fluid (STF) composed of sodium chloride (0.670 g), sodium bicarbonate (0.200 g), and calcium chloride dehydrate (0.800 g) in 100 ml of distilled deionized water was used for wettability study. The contact angle of inserts was measured by Half-Angle™ technique using a contact angle meter (CAM-PLUS MICRO model, Tantec INC, IL). A small amount of STF was placed on the insert with a microsyringe needle. The contact angle is measured immediately from the image of the drop projected on the screen [199]. Ten measurements were taken and the average was reported. The figure below shows the details (Figure 3.2).

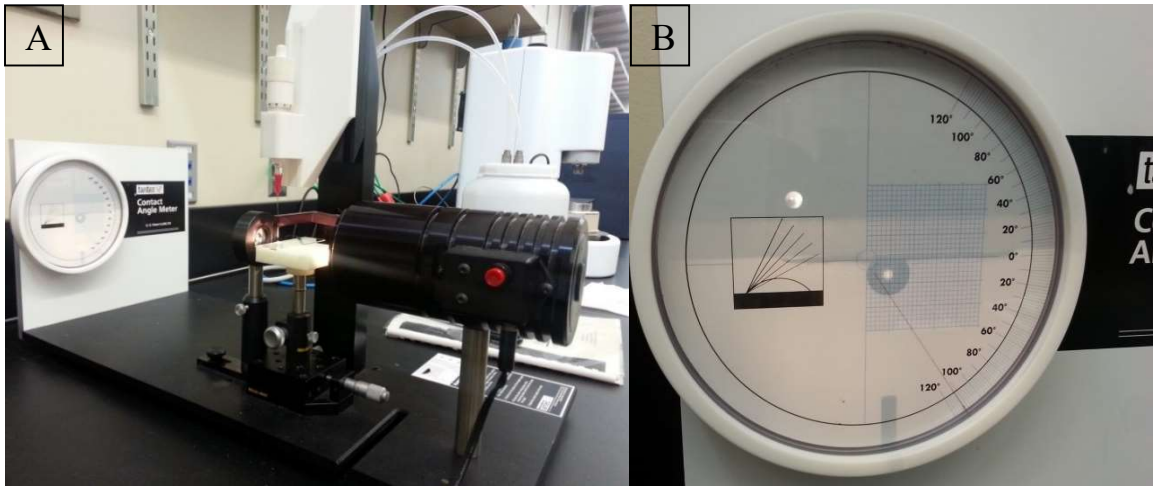

Figure 3-2: (A) Contact angle meter, CAM-PLUS MICRO, (B) Contact angle measurement process

3.3.8 In vitro drug release study

In vitro release of dexamethasone was performed using Franz diffusion cells with 2 cm^2 diffusion window across the dialysis membrane (Fisherbrand® Dialysis tubing, MWCO: 12,000-14,000 Da, 0.45 µm pore size). Phosphate buffer (pH 7.4) with 0.025% w/v of Tween 80 was used in the receptor compartment and stirred continuously with a magnetic bead at 125 rpm. Tween 80 was used to maintain the sink conditions. The temperature of receptor chamber was maintained at 34±0.5°C by circulating water bath [200, 201]. Precautions were taken to avoid air bubbles in the receptor chamber. Dexamethasone loaded inserts were placed in the donor compartment and wetted with 100 µl of phosphate buffer to simulate the wetting of inserts in the eye. The donor and receptor chamber openings were occluded with parafilm tape to prevent any evaporation. At regular time intervals, 300 µl of receptor fluid was withdrawn and replaced with an equal volume of fresh buffer. The samples were analyzed using HPLC for drug content. The Franz Diffusion cell setup mounted on magnetic stirrer is shown in figure 3.3.

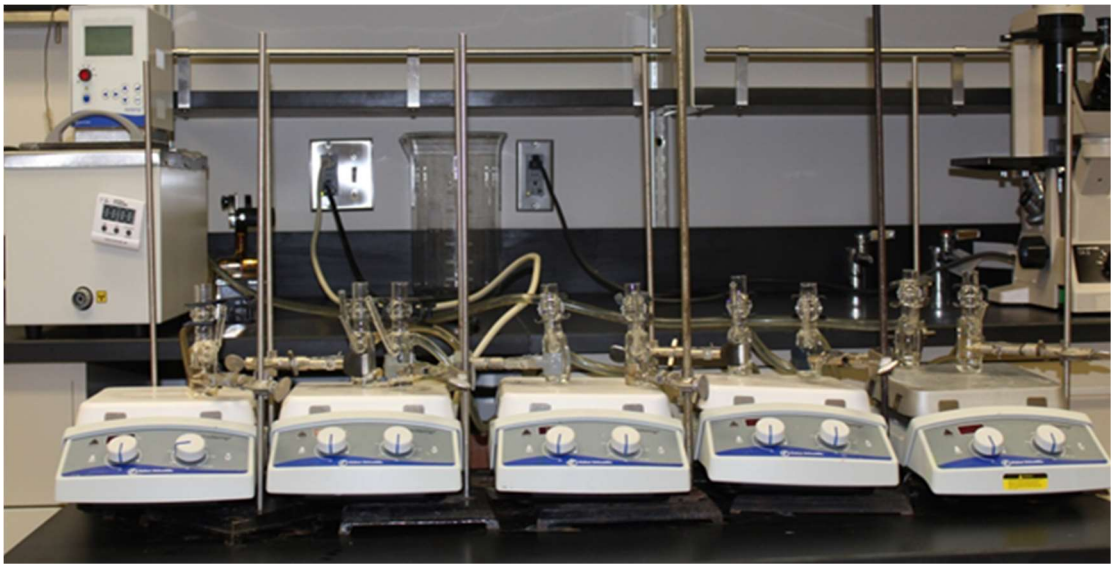

Figure 3-3: Franz Diffusion cell setup for *in vitro* drug release study

3.3.9 Fourier Transform Infrared Spectroscopy (FTIR)

A Thermo Scientific NICOLET iS5 Fourier Transform Infrared Spectrometer (iD3 ATR) equipped with Zinc-Selenium crystal for mounting the samples was used for obtaining the IR spectra of dexamethasone, PLA, PVA, blank and drug-loaded polymer inserts. The scanning range was from 400-4000 cm^{-1}. Thermo Scientific™ OMNIC™ was used for analyzing the peak.

3.3.10 Differential Scanning Calorimetry (DSC)

Thermal properties of inserts were analyzed with 822e Mettler Toledo DSC equipped with a TS0800GCI gas flow system connected to nitrogen gas supply. Dexamethasone, PLA, PVA, blank and drug-loaded polymer inserts were heated till 300°C at a ramping rate of 10°C/min using the 20 ml/min flow of nitrogen gas. Star-e software V 8.10 was used to obtain and evaluate the thermograms.

3.3.11 Scanning Electron Microscopy (SEM)

A JEOL JSM-7500F Scanning Electron Microscope (Peabody, USA) was used to check the surface morphology of inserts. The samples were attached to the double sided adhesive tape which was then attached to a stub. The samples were gold coated by putting the stub in the Denton Vacuum Desk II Sputter coater instrument. The coated samples were then observed at suitable accelerating voltage.

3.3.12 X-ray diffraction (XRD)

X-ray diffraction pattern for dexamethasone and inserts were taken using PANanalytical X-pert pro, Tokyo, Japan. The X-ray diffraction study was performed at 2theta (2θ) value of 0 to 50°.

3.3.13 Nuclear Magnetic Resonance (NMR) for estimating chloroform and DMF

The choloroform and DMF content was assessed in 10% dexamethasone loaded ENI and SCI. A 600 MHz Varian NMR Spectrometer was used with deuterated DMSO to obtain the NMR spectra for inserts. The chemical shift of hydrogens of dimethylformamide and chloroform were identified as published in the literature [202]. The peaks were integrated to obtain the area of the peaks relative to a standard/known hydrogen peak.

3.3.14 Cytotoxicity study

3.3.14.1 Harvesting bovine corneal endothelial cells

Bovine corneal endothelial cells were used for the cytotoxicity study of inserts. The bovine eyes were obtained from a nearby slaughterhouse (Kastel's Slaughter House and Processing Center, Riga, MI). The bovine eyes were obtained from the freshly slaughtered cows and the study was initiated immediately with 3-4 hours. The eyes were placed in the phosphate buffer before harvesting corneal cells as per the published procedure [203]. The cells obtained after harvesting were plated in a sterile petri dish with Dulbecco's modified

Eagle's medium (DMEM), 10% Fetal Bovine Serum (FBS) and 100 µg/ml penicillin-streptomycin solution and were incubated at 37°C for 24 hours. The nutrient medium (DMEM-F12) was replenished once every two days until the cells were confluent. The confluent cells were harvested and the final cell concentration was adjusted to 2 x 10^6 cells/ml.

3.3.14.2 Cytotoxicity study

Approximately 15000 cells/well were added to each well of a 96-well plate (Corning, Inc. NY). The plate was then incubated at 37°C in a 5% CO_2 environment for 24 hours to assist with cell attachment. After incubation, media from wells was removed with a pipette and cells were treated for another 24 hours with 200 µl of DMEM medium (negative control), DMEM with 5% DMSO (positive control), DMEM exposed to blank and DMEM exposed to drug-loaded inserts (10% dexamethasone loaded ENI and SCI). After 24 hours, the media were removed and fresh DMEM media with 10% MTT reagent was added to the wells. The cells were then incubated at 37ºC for 2-3 hours. The medium was removed and 150 µl of 100% DMSO was added to each well to allow the dissolution of the formazan salt formed. The absorbance of the wells was measured using a microplate reader at 570 nm to determine the cytotoxicity of each sample.

3.3.15 Sterility Validation Test

Sterility test was performed in order to verify the suitability of sterilization method to produce microbe-free sterile inserts. Inserts were sterilized by exposing them to UV light

on both sides for 10 minutes on each side. Glassware used in the test was autoclaved and all non-autoclavable materials were disinfected with isopropyl alcohol. Sterility testing was performed using plate and direct/tube inoculation [USP <71>] methods as per our published protocol [180, 204]. Tryptic soy broth (TSB) was used as a growth medium for direct/tube inoculation method. Liquid culture of *Staphylococcus aureus* Rosenbach ATCC BAA 1692 was grown in TSB medium for 24 hours, in a shaking water bath maintained at 37°C. A final concentration of 102 CFU/ml of microbes was obtained after a serial dilution with autoclaved sterile water. The concentration was determined using Spectronic 20 Genesys spectrophotometer (Spectronic Instruments, USA) using autoclaved sterile water as blank and was compared to McFarland standard no. 1 with a concentration of 3×10^8 CFU/ml. For direct inoculation method, the samples were labelled as negative control, positive control, positive sample control, and sterile sample vials based on the presence/absence of microbes. The negative control vial contained 9 ml of un-inoculated medium and 1 ml of sterile water. The positive control vial contained 9 ml of un-inoculated medium and 1 ml of solution containing 102 CFU/ml. The positive sample control vial contained 9 ml of un-inoculated medium, non-sterile insert and 1 ml of solution containing 102 CFU/ml. The sterile sample vial contained 9 ml of un-inoculated medium, sterile insert and 1 ml of sterile water. All vials were tested in duplicate and incubated at 37°C to speed up the growth of bacteria.

Table 3.1: Contents of each sample

Negative control	**Positive Control**	**Positive Sample**	**Sterile Sample**
9.0 ml un-inoculated medium + 1.0 ml sterile water	9.0 ml of un-inoculated medium + 1.0 ml liquid with 102 CFU/ml of microbes	9.0 ml of un-inoculated medium +1.0 ml liquid with 102 CFU/ml of microbes + non-sterile sample	9.0 ml un-inoculated medium + 1.0 ml sterile water + sterile sample

For the plate inoculation method, 100 µl samples were withdrawn from the vials prepared by the direct inoculation method on days 0, 7 and 14. These samples were streaked on sterile Mueller Hinton (MH) agar plates which were then incubated at 37°C for 24h. The plates were visually checked for bacterial growth.

3.4 Results

Dexamethasone loaded inserts with varying concentrations drug concentrations of 1%, 5% and 10% were prepared using electrospinning and solvent casting methods. A 2:1 ratio of PLA: PVA was used in the preparation of inserts. The inserts obtained after electrospinning were homogenous, smooth, uniform and white in color, while those obtained from solvent casting were rough, porous, brittle and white in color with nonhomogeneous appearance.

Figure 3-4: (A) Electrospun nanofiber inserts, (B) Solvent cast inserts

Inserts containing 50 µg of dexamethasone were cut and used for the physicochemical characterization. ENIs were easily foldable and tend to stick to the surfaces because of static charge, while solvent cast were brittle and uncharged. The change in the pH of STF did not vary significantly in the presence of inserts for up to 8 hours. Table 3.1 summarizes the physicochemical parameters of the inserts.

Table 3.2: Summary of film thickness, drug loading, drug content, contact angle and pH change in STF

Preparation method	**Percent Drug loading**	**Film Thickness (µm)** (Mean ± SEM)	**Drug Content (%)** (Mean ± SEM)	**Contact Angle (°)**	**pH Change**
Solvent cast	1%	225.8±0.02	103±1.79	101.6±10.9	<1
	5%	227.5±0.002	108±10.5	100±5.8	
	10%	322.5±0.03	104±7.3	97.6 ± 10.5	
Electrospun	1%	50±0	119±2.7	108.4±4.8	<1
	5%	62.5±0	102±10.7	104.8±4.4	
	10%	93.3±0.06	104±2.2	107.3 ± 6	

NP: Not Performed

The thickness of inserts increased from 225.8±0.02 µm to 322.5±0.03 µm and 50.0 ±0.0 µm to 93.3±0.06 µm with an increase in the drug loading from 1% to 10% in both solvent-cast and electrospun methods, respectively. The overall thickness of ENIs was found to be 3-5 times lower than the SCIs. The contact angle of the SCIs with STF was between 97.6 ± 10.5° to 101.6±10.9° while that of ENIs was between 104.8±4.4° to 108.4±4.8°.

The HPLC method for quantification of dexamethasone concentration was successfully developed and validated for linearity, accuracy, limit of detection (LOD), limit of quantification (LOQ), and precision. The retention time of dexamethasone was found to be

about 2.9 minutes at the absorption wavelength of 242 nm. The calibration curve resulted in a straight line (y = 1991x + 767) with a correlation coefficient value (R^2) of 1, Limits of detection and quantification were found to be 0.533 ng and 1.616 ng, respectively. The percentage recovery of dexamethasone ranged from 97.1%-100.2%, indicating the method accuracy. The developed method also showed a good intra-day precision and suitability with relative standard deviation (RSD) less than 2%. Calibration curve of dexamethasone is shown in figure 3.5 and the chromatogram of dexamethasone is shown in figure 3.6.

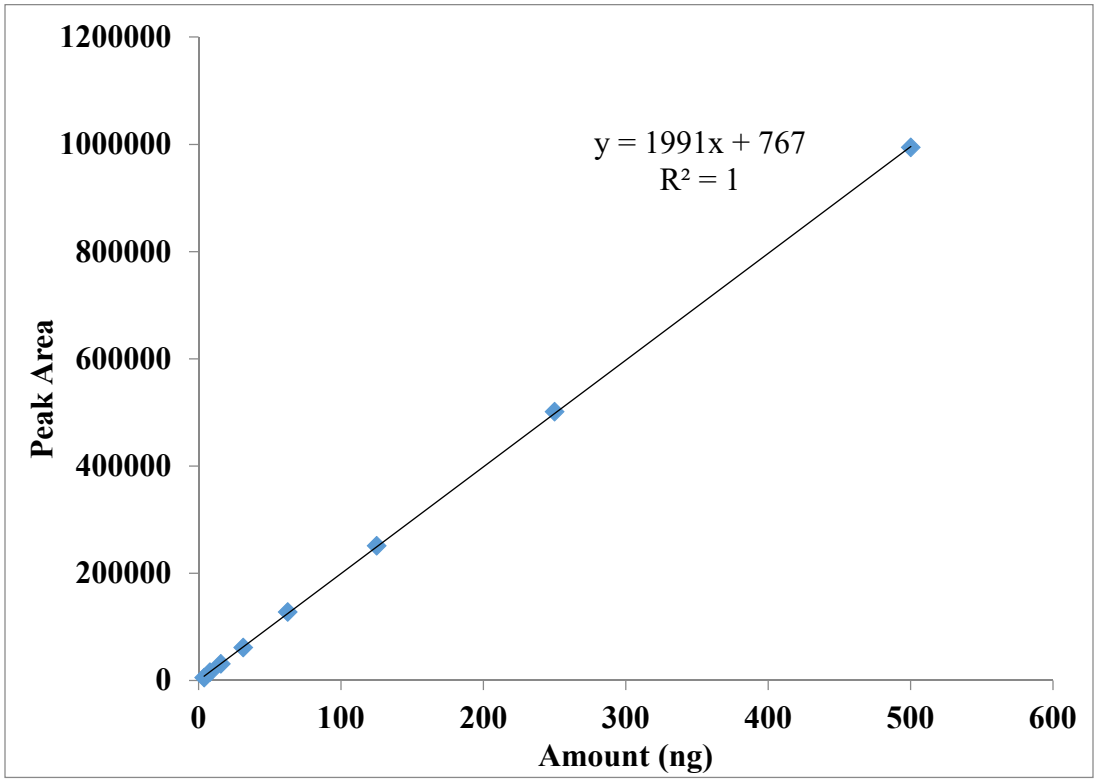

Figure 3-5: Calibration curve of dexamethasone

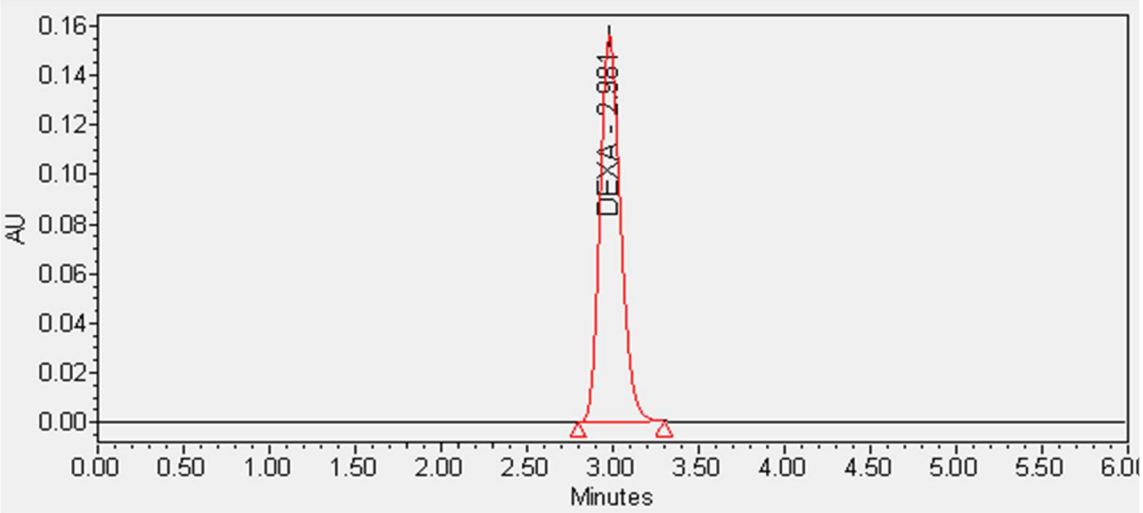

Figure 3-6: HPLC chromatogram of dexamethasone

The drug content of SCIs and ENIs were found to be in the range of 103±1.79% to 108±10.5 % and 102±10.7 % to 119±2.7 % respectively (Table 3.1). The drug content was found to be more uniform for ENIs compared to SCIs.

In vitro drug release profile of the ENIs showed a first order release rate of 0.62 µg/h, 1.46 µg/h and 2.30 µg/h for 1%, 5% and 10% inserts respectively while SCIs followed no particular release model. In case of ENIs, 1% dexamethasone loaded inserts completely released the drug in 4 hours, while 5% and 10% released in 24 hours and 36 hours respectively (Figure 3.7). In SCIs, there was no definite change in release behavior of the insert with change in drug loading (Figure 3.8). The error bars in ENIs are smaller representing the consistent and predictable release of the drug from inserts.

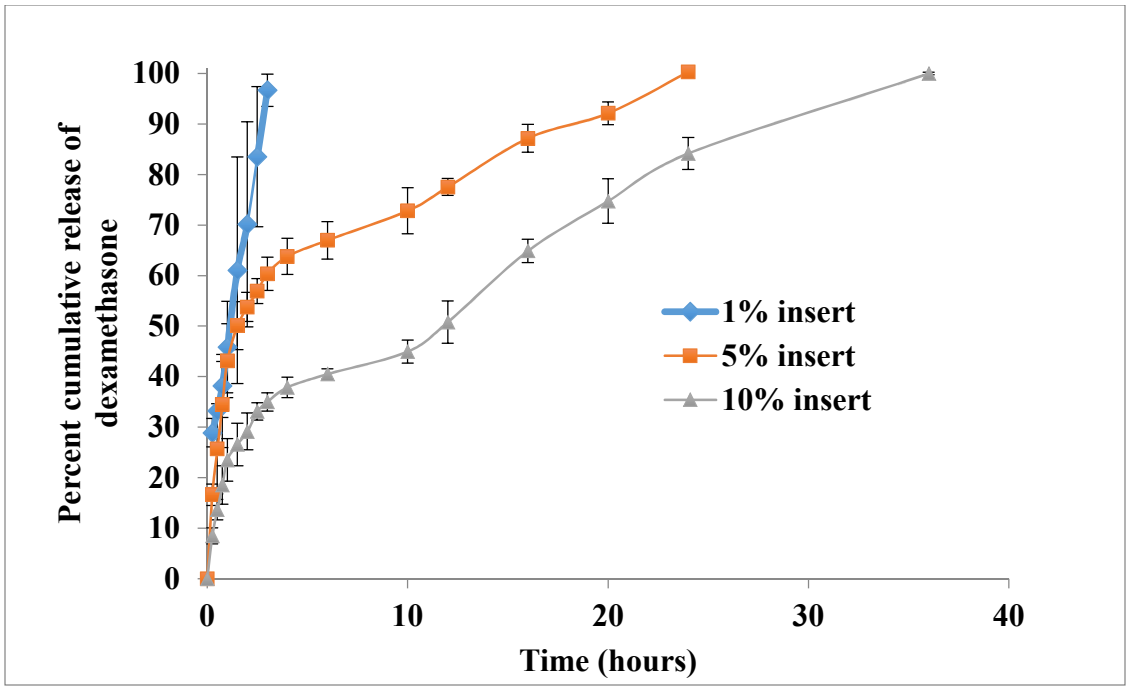

Figure 3-7: *In vitro* release of dexamethasone from ENIs

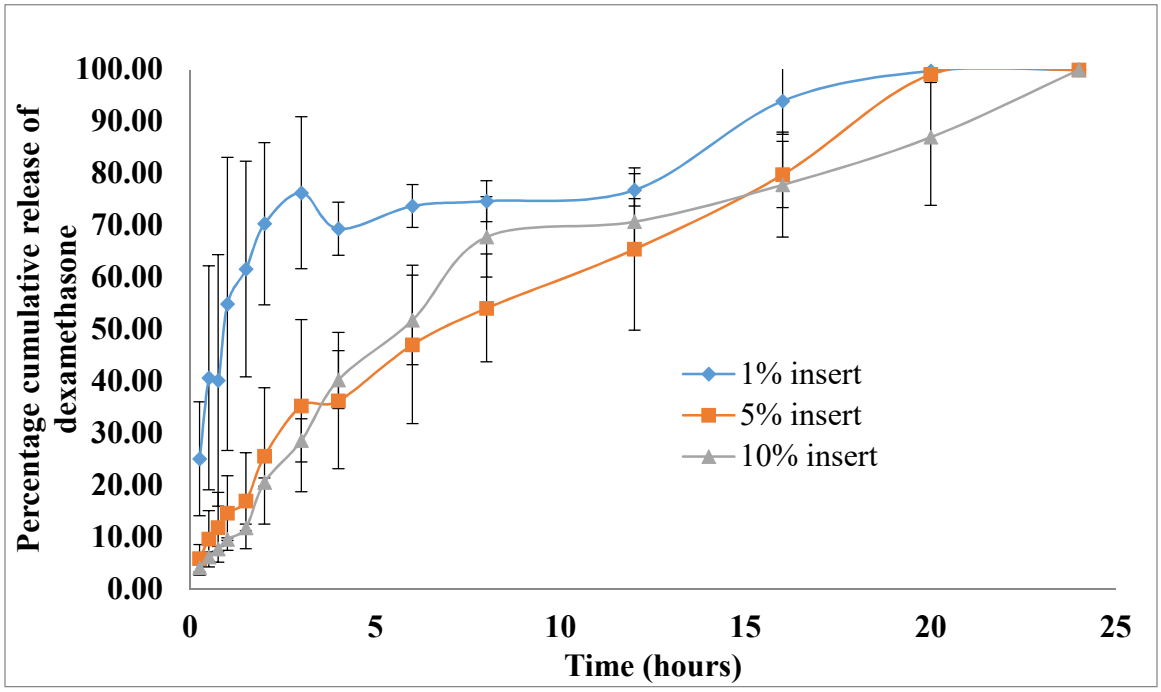

Figure 3-8: *In vitro* release of dexamethasone from solvent cast inserts

FTIR spectrum of dexamethasone showed characteristics absorption peaks at 3467 cm^{-1} and 1270 cm^{-1} which are due to –O-H stretch and C-F stretch respectively [205] and other peaks at 2988.73 cm^{-1}, 1701.47 cm^{-1}, 1658.46 cm^{-1}, 1610.10 cm^{-1} were due to -C-H stretch, C20 ketone stretch, -C=C and C3 ketone groups, respectively (Figure. 3.9). FTIR spectra of ENIs and SCIs are shown in Figs. 3.10 and 3.11, respectively. In case of SCIs and ENIs, the major peaks observed in the spectrum of the inserts are due to either PLA or PVA. The peak at 2850 - 3000 cm-1 is attributed to C-H alkene stretch in PLA and specific peak at ~1750 cm^{-1} is due to the carbonyl stretch in the same molecule [206]. The characteristics absorption signal of PLA is observed at ~1090 cm^{-1}[207]. This can be comparatively observed in figure 3.12.

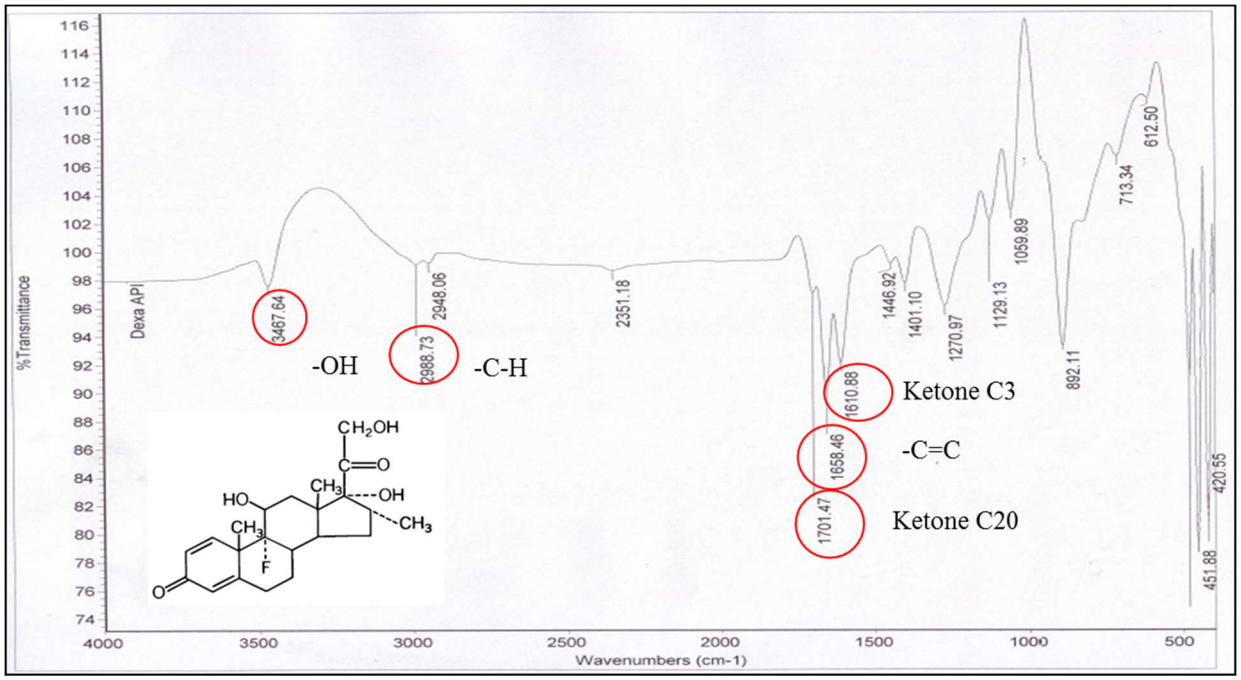

Figure 3-9: FTIR spectrum of dexamethasone

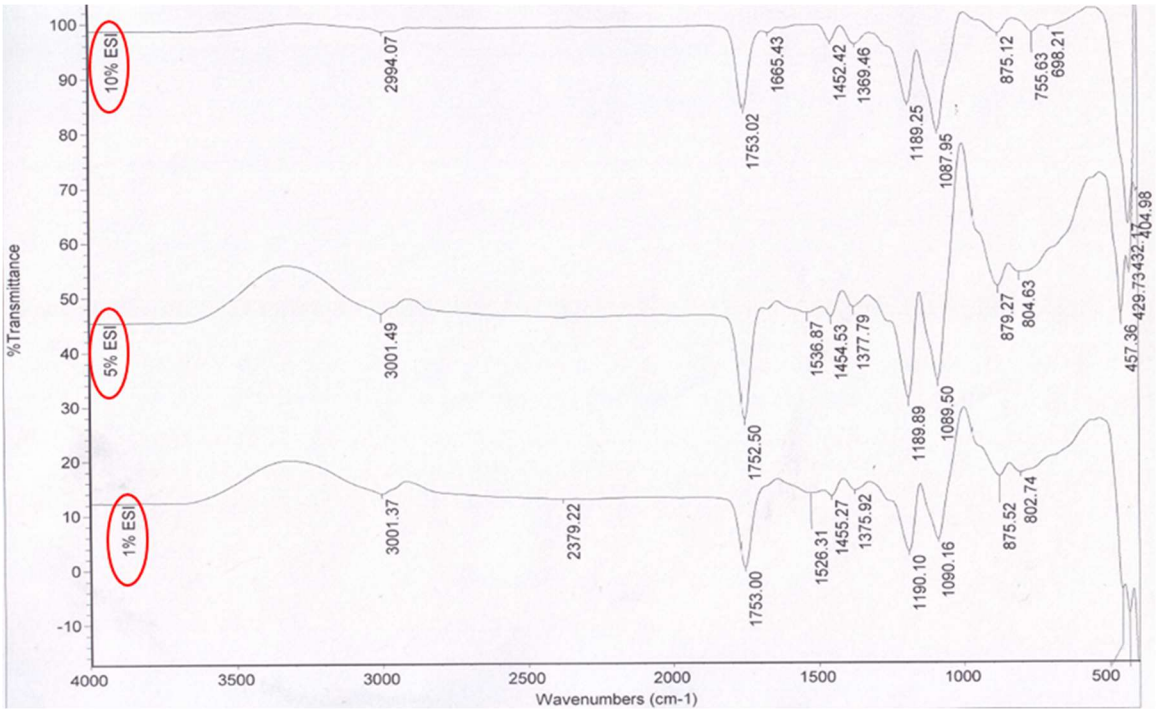

Figure 3-10: FTIR spectra of dexamethasone loaded electrospun nanofiber inserts

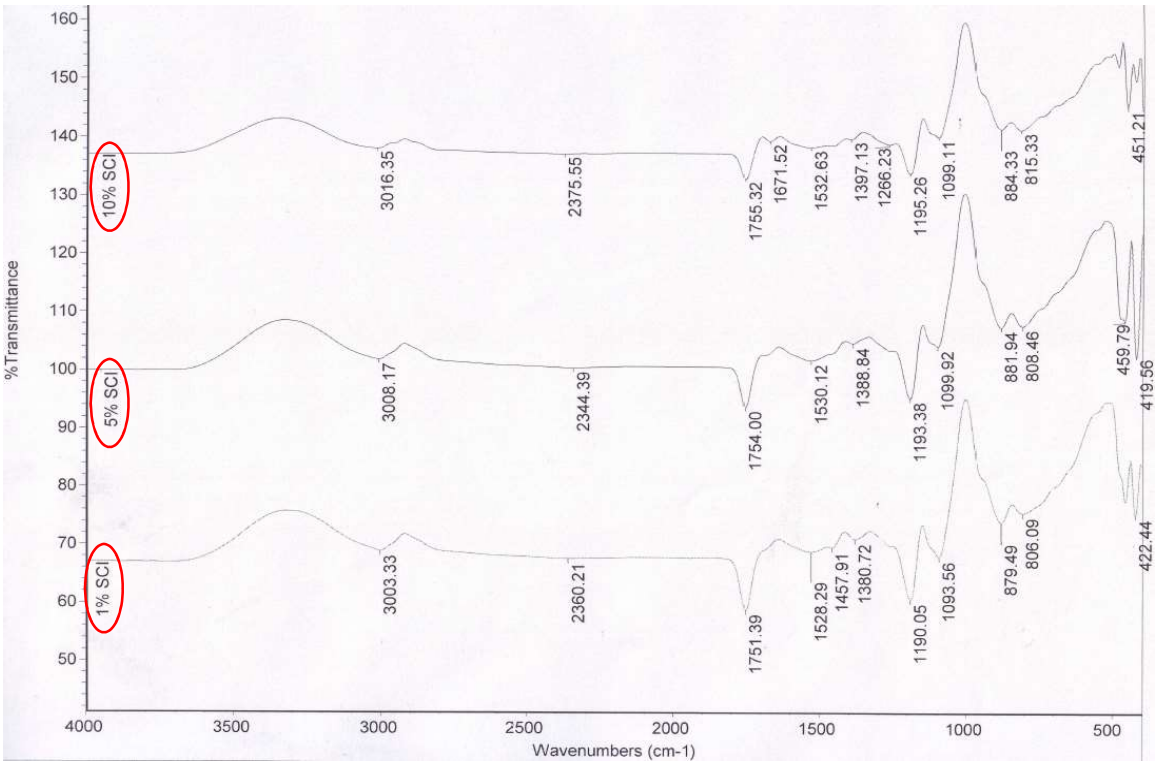

Figure 3-11: FTIR spectra of dexamethasone loaded solvent cast inserts

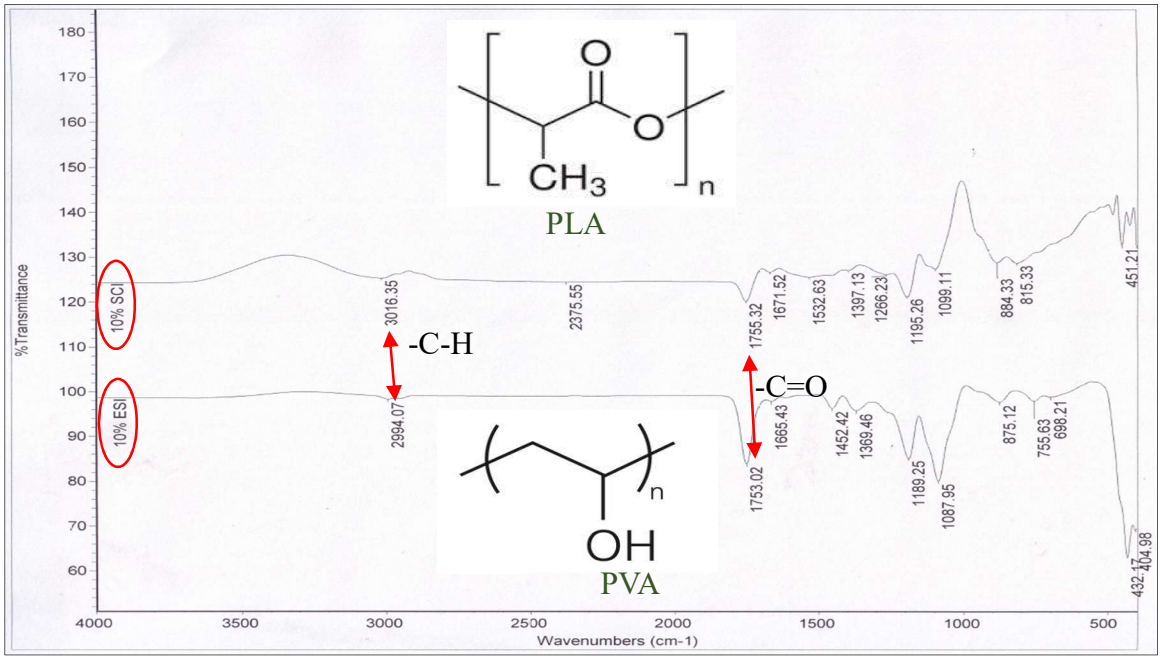

Figure 3-12: FTIR spectrum comparison between 10% dexamethasone loaded inserts prepared using solvent cast and electrospinning techniques.

DSC thermogram of dexamethasone exhibited characteristic endothermic peak with an onset at 243°C and peak temperature of 272°C, which corresponds to its melting point [208]. Blank ENIs showed a glass transition of PLA between 60ºC -70°C [53] and a melting endotherm peak in between 160ºC – 170ºC [53, 209], while PVA exhibited an endotherm peak with an onset at 240°C and a peak temperature of 246°C corresponding to its melting point [210]. DSC thermograms with 1%, 5%, and 10% dexamethasone ENIs have shown a similar trend. They all showed a prominent peak for PLA at 165°C; however, the expected dexamethasone peak became less noticeable with 1%, 5% and 10% drug loaded inserts, which indicated the absence of the crystalline form of dexamethasone (Figure 3.13). The thermograms of SCIs had the same thermal events like that of ENIs indicating the absence of the crystalline form of dexamethasone (Figure 3.13).

The surface morphology of ENIs was evaluated using SEM. Figure 3.14 shows the SEM images of ENIs and 10% dexamethasone loaded SCI. The ENIs showed very thin, uniform fibers in the nanometer size range, which are consistent with increasing concentration of dexamethasone. While SCI with 10% dexamethasone showed a variable surface morphology with non-uniform pores, crevices and surface deformations. This could be due to non-uniform drying of the SCI.

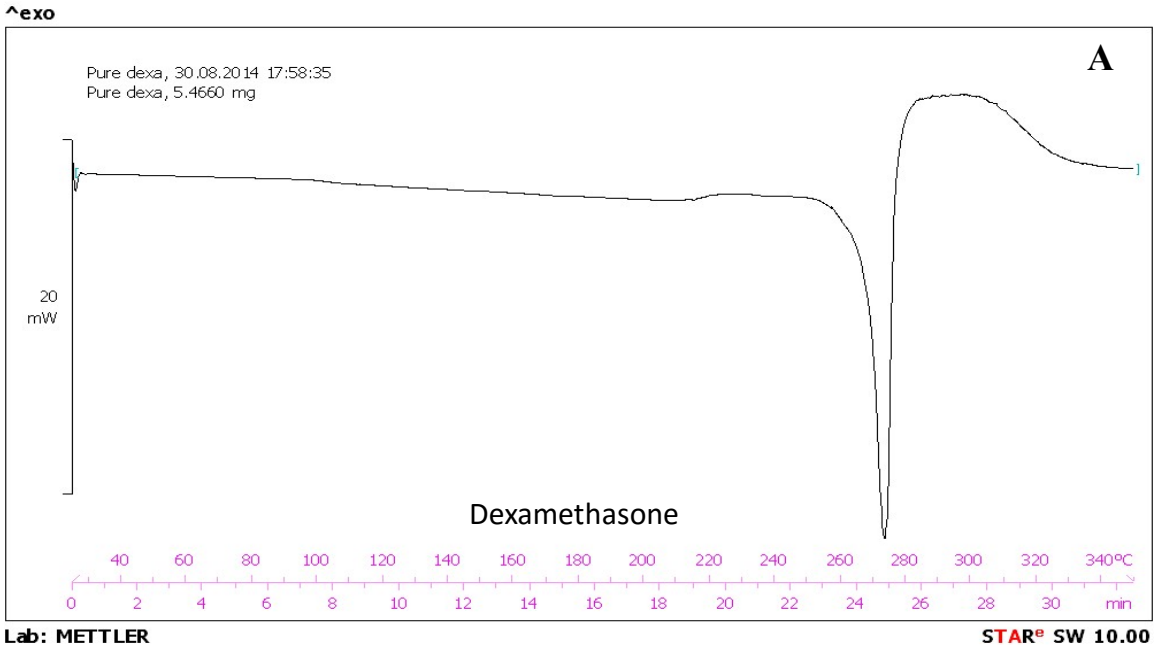

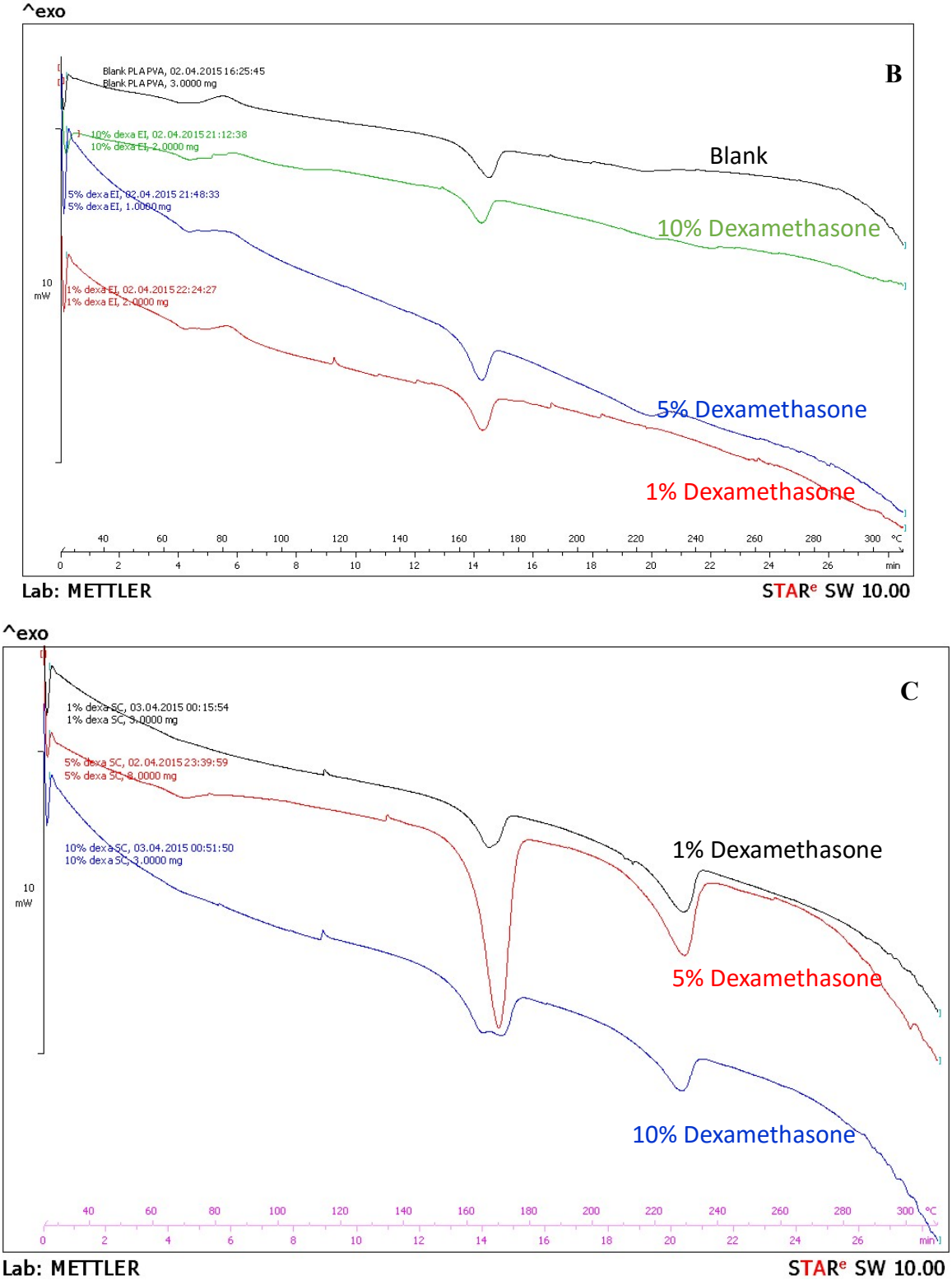

Figure 3-13: DSC thermogram of (A) Pure dexamethasone, (B) electrospun inserts (C) solvent cast inserts

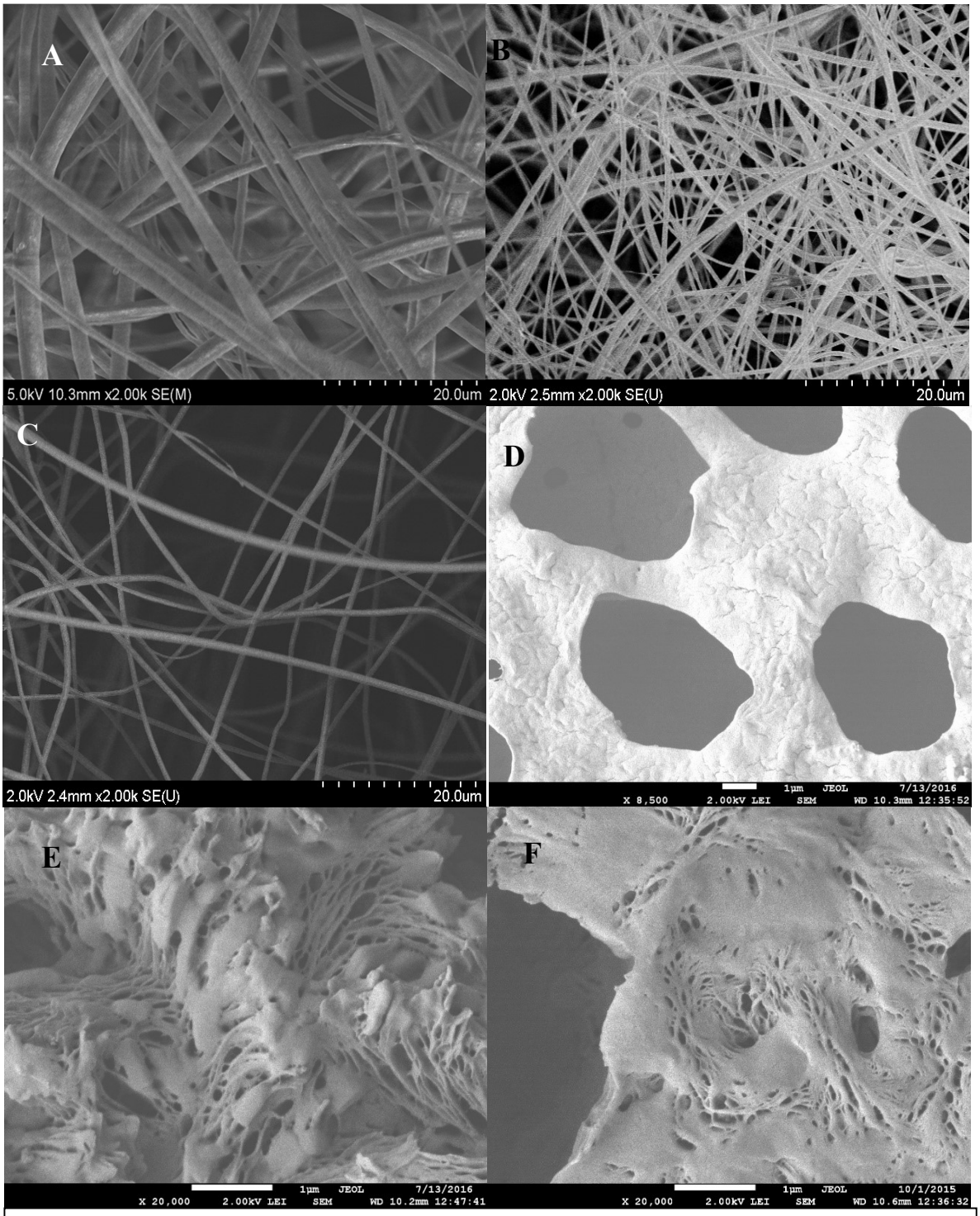

Figure 3-14: Scanning electrospun microscopy images of inserts. Electrospun inserts of 1% dexamethasone (A), 5% dexamethasone (B), 10% dexamethasone (C). Solvent cast insert of 1% dexamethasone (D), 5% dexamethasone (E), 10% dexamethasone (F).

X-ray diffraction pattern of the ENIs showed that all samples were devoid of any crystalline form of dexamethasone and PLA polymer as reported in literature [211]. SCIs present peaks at 16.8° and 19.5°, which are characteristics of PLA crystals. The intensity of the peak indicates small fraction of semi-crystalline PLA, which is also reported in the literature [212, 213]. In addition, the peak representing the semi-crystalline nature of PVA fibers is observed at 19.7°, which was merged with the PLA peak [214, 215]. The resulting x-ray diffraction pattern is the combined effect of both the polymers. Absence of any dexamethasone peaks further proves that the drug was part of the polymeric matrix. Figure 3.15 shows the x-ray diffraction patterns of electrospun inserts (A), solvent cast inserts (B) and dexamethasone (C).

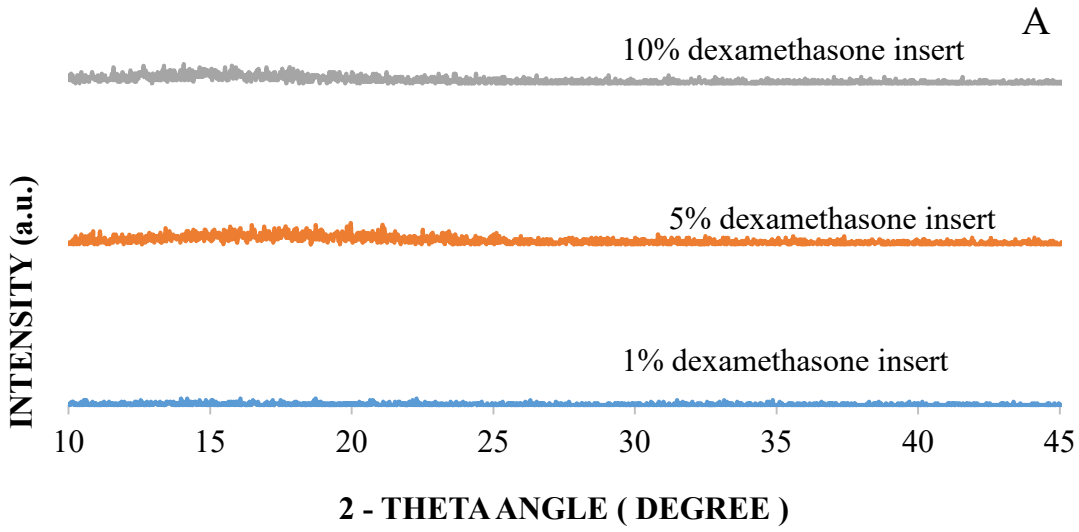

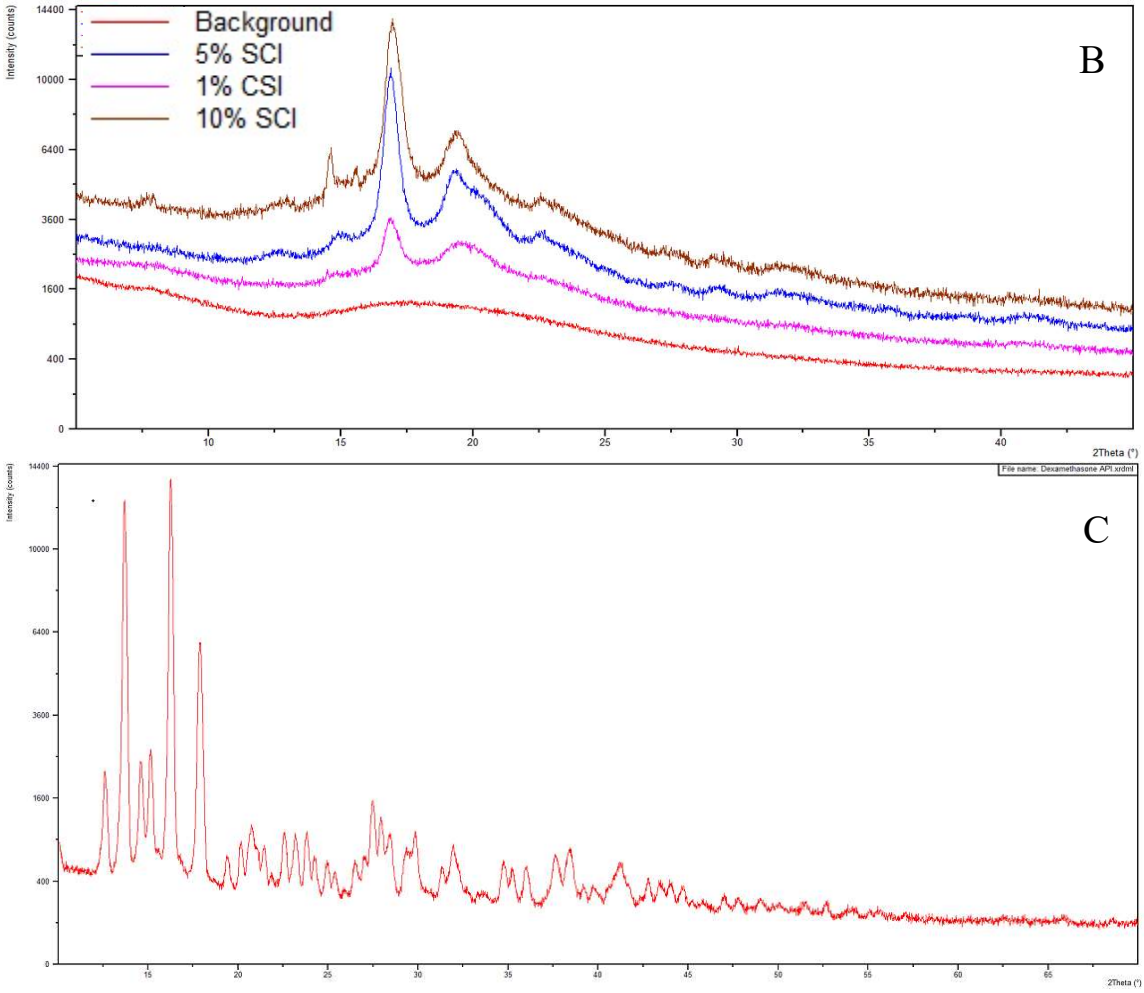

Figure 3-15: X-ray diffraction pattern of electrospun nanofiber inserts (A), solvent cast inserts (B) and dexamethasone (C)

Based on the above studies, 10% dexamethasone loaded ENI was considered optimum and further characterized for chloroform and DMF content, cytotoxicity and sterility. SCI containing 10% dexamethasone was used as a control. The chloroform and DMF content was analyzed for 10% drug loaded inserts prepared using both methods. NMR spectra obtained for the ENI and SCI were integrated against the C4-H peak of dexamethasone obtained at 6.2 ppm [202, 216]. The NMR spectra are shown in figure 3.16. There were no

quantifiable peaks at the chemical shift value equivalent to the hydrogen of chloroform. This indicates the absence of chloroform in the inserts. By taking C4-H of dexamethasone as the reference peak (100%), the peak at the chemical shift equivalent to hydrogen of DMF was quantified. The DMF quantity in ENI and SCI was found to be 0.007 % (w/w) and 0.123% (w/w), respectively.

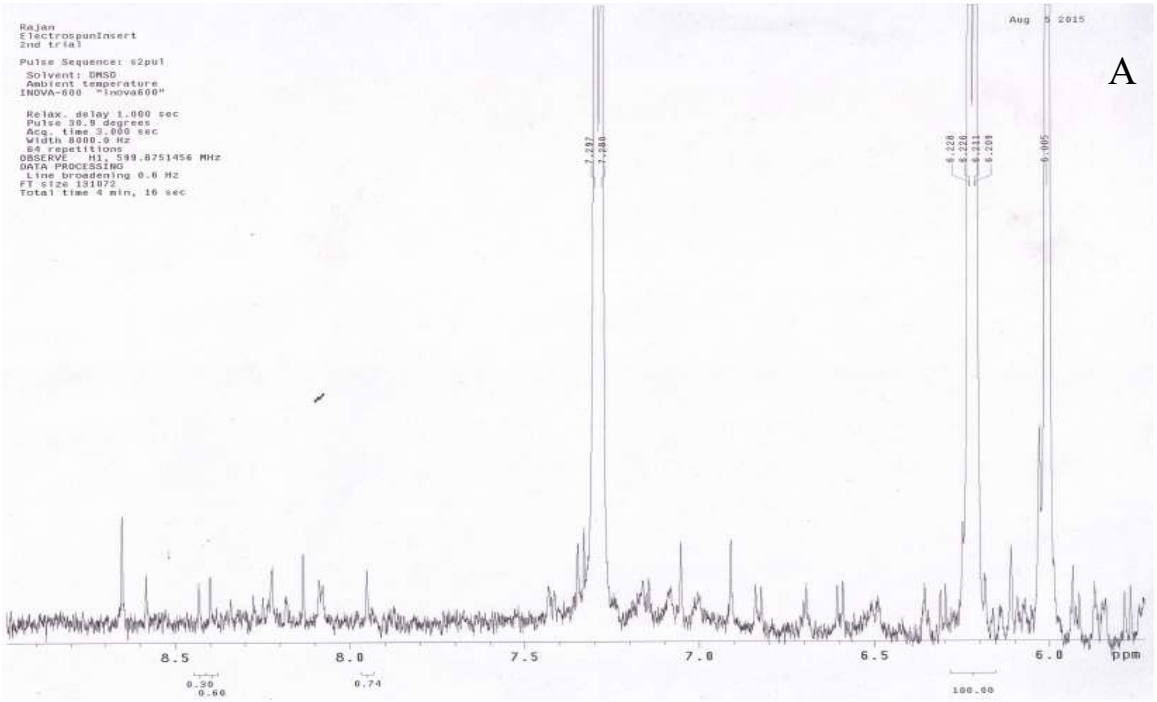

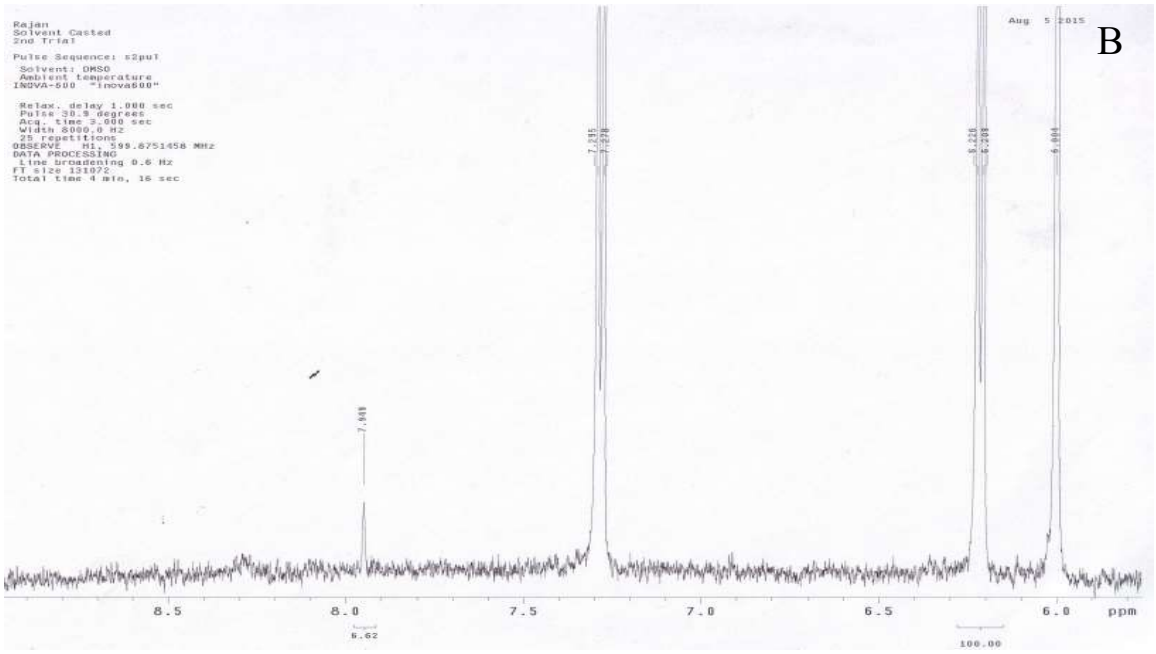

Figure 3-16: NMR spectrum of 10% dexamethasone loaded electrospun nanofiber insert (A) and solvent cast insert (B)

The cytotoxicity of the 10% drug loaded ENI and SCI was compared with blank inserts in bovine corneal endothelial cells. In the presence of 20% DMSO, as a positive control, only 31% cell viability was observed. As shown in the figure 3.17, the percentage cell viability of electrospun blank and drug loaded, solvent cast blank and drug loaded inserts were approximately 115%, 115%, 118% and 124%, respectively. This indicates that the inserts were not toxic in bovine corneal endothelial cells for up to 24 hours.

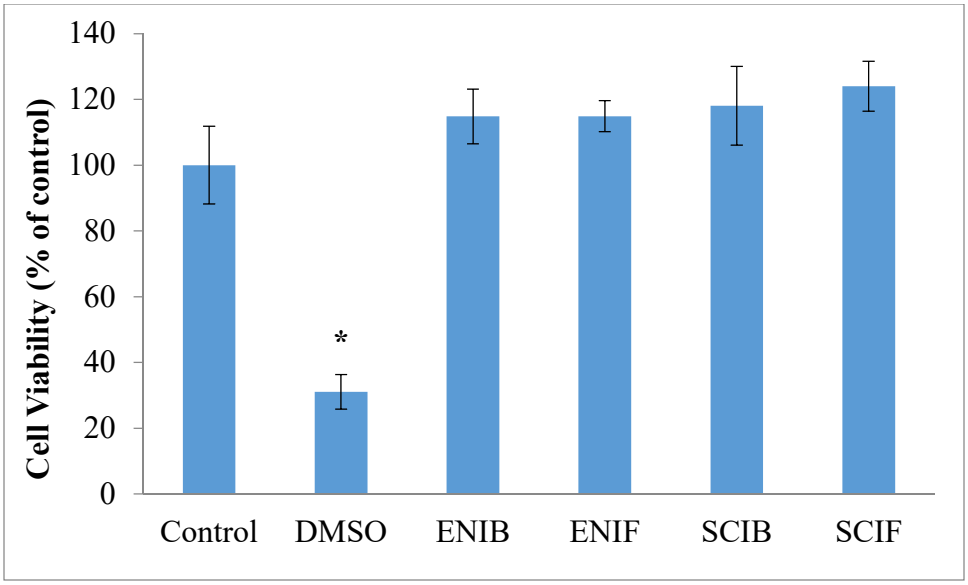

Figure 3-17: Cell viability of electrospun blank (ENIB), electrospun formulation (ENIF), solvent cast blank (SCIB) and solvent cast formulation (SCIF) compared with negative control (Control) and positive control (DMSO). $^{*}P < 0.05$

The verification of sterility of UV sterilized inserts was done by direct inoculation and the plate inoculation method in TSB broth. One hundred microliters of samples were withdrawn from the vials of direct inoculation method at 0, 7th and 14th days and streaked over Mueller-Hinton agar plates. The plates were then incubated at 37°C for 42 hours and checked for the growth. The results are shown in table 3.2. The plates with sterile samples and negative control showed no bacterial growth, while plates with positive control and positive samples showed bacterial growth. Similarly, the tubes containing positive control and positive sample did not show any turbidity, while negative control and positive samples showed turbidity at 14th day due to microbial growth. This study concludes that UV sterilization can be used sterilization of the inserts and their sterility was maintained for at least 14 days (Figs 3.18 and 3.19)

Table 3.3: Sterility validation study: Results of plate inoculation study on a MH Agar plate indicating the presence (+) or absence (-) of microbial growth in 0, 7th and 14th day.

No. of days	Negative control	Positive control	Positive sample (ENI)	Positive sample (SCI)	Sterile sample (ENI)	Sterile sample (SCI)
0	-	+	+	+	-	-
7	-	+	+	+	-	-
14	-	+	+	+	-	-

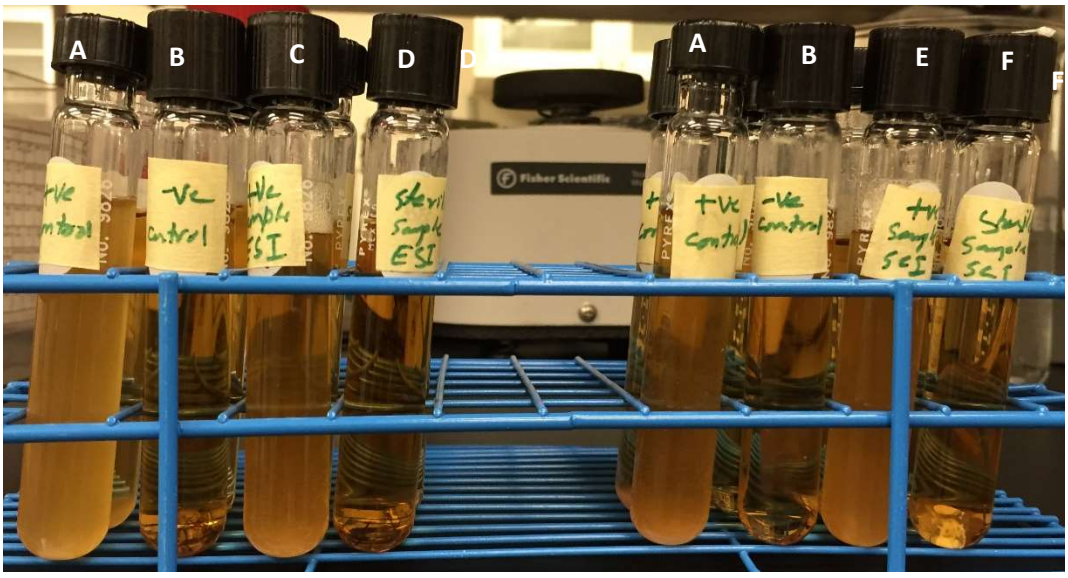

Figure 3-18: Direct Inoculation Method after 14 days: A- positive control, B- negative control, C- Positive sample (electrospun), D- Sterile sample (electrospun), E- Positive sample (solvent cast), F- Sterile sample (solvent cast)

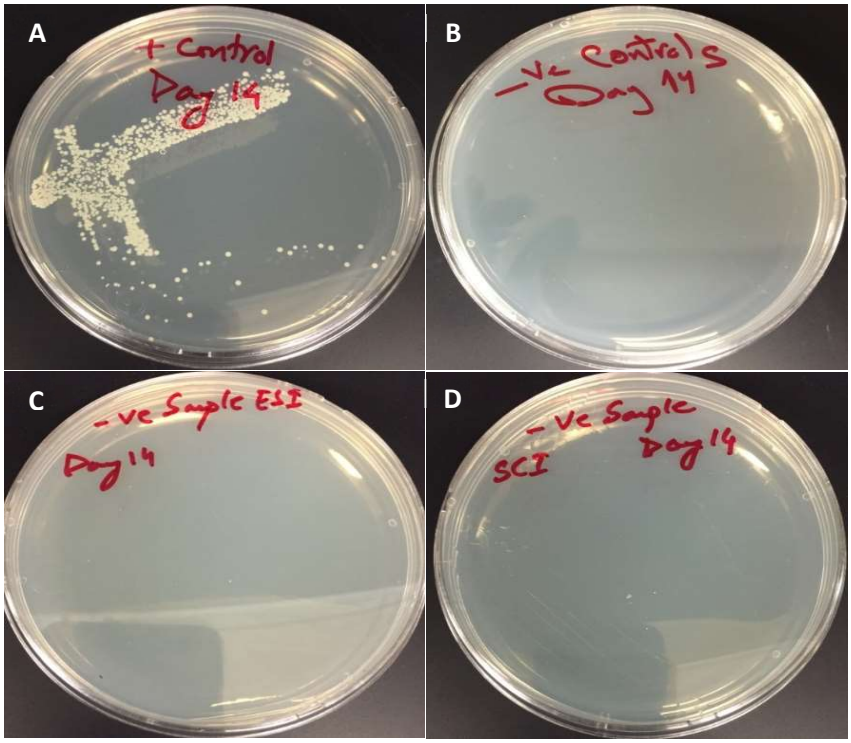

Figure 3-19: Petri plates inoculated with 14 days' samples of A- Positive control, B-negative control, C- sterilized electrospun insert, D- sterilized solvent cast insert

3.5 Discussion

In this work, we have successfully prepared different types of inserts loaded with varying concentrations of dexamethasone by two different methods, viz., electrospinning and solvent casting and characterized them *in vitro*. Electrospinning parameters, pump rate of syringe pump, the distance between the tip of the syringe and the collector plate and the applied voltage were optimized based on the past experience and by performing multiple trials. ENIs were found to be smooth, homogeneous and uniform. The smooth surface of ENIs would be favorable for the ocular use compared to non-homogenous and rough surface SCIs. The rough surface of SCIs was also evident from the SEM image. SCIs were found to be brittle and posed difficulty in handling. On the contrary, ENIs possessed good folding endurance and this makes the insert safe and comfortable for ocular use.

The thickness of SCIs ranged from 225.8±0.02 μm to 322.5±0.03 μm, while the thickness of ENIs ranged from 50.0 ±0.0 μm to 93.3±0.06 μm. The thickness of SCIs and ENIs increased with drug loading from 1% to 10%. This could be due to the increase in drug content. Ocular inserts reported in the literature showed a thickness of 0.070 - 0.500 mm. Both methods resulted in inserts with thickness values within the reported range in literature [184]. However, thinner inserts are desirable as they are easy to apply, cause less eye irritation and have no “foreign body sensation” [188]. No significant change in the pH of STF was observed in the presence of inserts. This is yet another required property of an insert in order to avoid irritation/discomfort resulting from pH fluctuations. Both techniques resulted in inserts with similar contact angle values around 100° indicating the

hydrophobic nature of inserts. This could be attributed to the presence of hydrophobic PLA polymer in the insert [217, 218].

The thermal events observed in the DSC study indicate that the dexamethasone is a part of the polymeric matrix and inserts are devoid of any free drug molecules in crystalline state. The endothermic event of dexamethasone at 272°C, corresponding to its melting point was missing in both types of inserts. The glass transition and melting of PLA occurred at 60°C - 70°C and 160 °C - 170°C, respectively. The melting of PVA happened at 140°C-150°C. There were no detectable interactions between the drug and the components of the inserts. The same was confirmed with the FTIR study where the characteristic peaks of the drug, 3467 cm^{-1} (-O-H stretch) and 1270 cm^{-1} (C-F stretch) were missing in the inserts. Though the interaction between the drug and the polymers were not evident in these studies, the possibility of minor interactions like hydrogen bond, van der Waals interactions cannot be excluded [219]. The ENIs showed very thin, uniform, porous fibers in the nanometer size range, while the SCIs showed a non-uniform surface with variable surface morphology, crevices and surface deformations. This could be due to non-uniform drying of the solvent from SCIs. The creation of the pores on ENI could be attributed to the difference in evaporation rates of chloroform (more volatile solvent) and DMF (less volatile solvent). As the nanofibers fly towards the collector, chloroform starts to evaporate faster than the less volatile solvent DMF. This difference in the rates of evaporation of chloroform and DMF results in cooling effect and condensation of water vapor into water droplets on the fibers. DMF mixes well with the water droplets on the inner and outer surfaces of the fibers

and the gradual evaporation of water droplets and the solvents result in the formation of pores in the nanofibers [220].

X-ray diffraction pattern of ENIs did not show any crystalline peaks of dexamethasone, PVA and PLA polymers. As reported in the literature, the thin uniform fibers of electrospun mats are devoid of any PLA or PVA peaks, while the SCIs showed semi-crystalline peaks [212, 213]. The 2θ value of the peaks in SCIs match with the peaks observed for PLA (16.8° and 19.5°) and PVA (19.7°) polymers. Such semi-crystalline nature could be attributed to multi-layered and rough surface morphology of SCIs, giving it pellet characteristics rather than the properties of a thin uniform film [213]. This hypothesis is further backed by the SEM study of the inserts. The surface morphology of ENIs showed the presence of smooth, uniform, non-beaded, nanofibers, while the solvent casting technique produced inserts with rough, and non-uniform surface. *In vitro* release behavior suggested a uniform and predictable release of dexamethasone from ENIs for up to 36 hours, while SCIs exhibited an erratic and unpredictable release behavior. This behavior is undesirable of inserts and make them unreliable for drug delivery application. ENIs showed a first-order release rate of 0.62 µg/h, 1.46 µg/h and 2.30 µg/h for 1% (w/w), 5% (w/w) and 10% (w/w) dexamethasone loaded inserts, respectively. Based on the *in vitro* release, 10% dexamethasone loaded insert prepared using electrospinning technique was considered optimum and characterized for residual organic solvents, cytotoxicity and sterility following exposure to UV light. The results were further compared with 10% dexamethasone loaded insert prepared using the solvent casting technique.

NMR was used to assess and compare the amount of residual organic solvents present in 10% dexamethasone loaded ENI and SCI. Chloroform is a volatile solvent with a boiling point of 61°C [221]. Chloroform was easily removed from both types of inserts, while DMF being a solvent with high boiling (~156°C) could not be fully removed [222]. This was apparent in NMR quantification where chloroform was not detected but DMF content was 0.007% (w/w) and 0.123 % (w/w) in electrospun and solvent cast inserts, respectively.

Based on the hepatotoxic effects of DMF, the Occupational Safety and Health Administration's (OSHA) permissible exposure limit (PEL), the NIOSH recommended exposure limit (REL), and the threshold limit value (TLV) of the American Conference for Governmental Industrial Hygienists (ACGIH) for DMF, are all 10 ppm as an 8-hour time-weighted average (TWA) with a notation that skin absorption can be significant [223]. Repeated oral doses of DMF at 450 mg/kg in rats produced reversible changes in body weight gain and liver injury. At DMF concentrations of 1,658 ppm or greater, sensory irritation was produced in the mouse [224]. DMF was reported to be irritating in rabbit eyes following administration of 0.1 ml twice at an interval of 5 minutes followed by brief irrigation with water. However, the eye returned to normal within a day or two. A 25% v/v of DMF in water did not produce any effects when injected into the conjunctival sac of the rabbit, while concentrations higher than 50% v/v produced slight to severe irritation [225, 226]. In the present study, the DMF content in the ENI was significantly lower than the SCI. Based on the scanty literature evidence regarding the toxicity of DMF in the eye, we do not anticipate any toxicity issue, especially with ENI. However, the use of alternative solvents that are safe is recommended in the preparation of ENIs.

The cytotoxicity of 10% dexamethasone inserts prepared using electrospinning and solvent cast techniques were further assessed in bovine corneal endothelial cells. The bovine corneal cells were obtained from a freshly slaughtered animal by using the published extraction procedure [203]. From the MTT assay method, we observed that the DMF was sufficiently low to be cytotoxic in cells. MTT is a colorimetric test which determines the cell viability based on cellular metabolic activity through NAD(P)H-dependent cellular oxidoreductase enzymes. The viable cells form purple colored formazan product after metabolizing tetrazolium salt present in the MTT reagent. The higher the absorbance value, the higher is the viable cell count and lesser is the toxicity. All the insert samples were found to be non-cytotoxic. As per USP guidelines, sterility is an important reuirement for ophthalmic preparations [227]. In the present study, UV light was used to sterilize the inserts. Later the inserts were tested for sterility as per the USP guidelines using plate and direct inoculation techniques. The inserts were found to be sterile for up to 14 days.

3.6 Conclusion

In the present study, we have prepared dexamethasone loaded PLA/PVA inserts by electrospinning and solvent casting methods and characterized them for suitability for ocular application. Our results indicate that ENIs of PLA/PVA perform better than inserts prepared by solvent casting technique and are capable of delivering drugs in a sustained fashion. ENIs were found to be distinctly superior to SCIs in terms of drug content uniformity, thickness, surface morphology, *in vitro* release profile and the presence of residual solvents. The 10 % (w/w) dexamethasone loaded ENI exhibited sustained release of the drug for more than 24 hours and could be used as a suitable alternative for treating

the anterior eye segment inflammatory diseases. Further studies in order to assess the toxicity and pharmacokinetics parameters of the ENI should be conducted in animals.

Acknowledgements

This work was supported by start-up funds from The University of Toledo and a grant from the deArce Memorial Endowment Fund in Support of medically related research.

References

1. Nayak, R., et al., *Recent advances in nanofibre fabrication techniques.* Textile Research Journal, 2011: p. 0040517511424524.
2. Greiner, A. and J.H. Wendorff, *Electrospinning: a fascinating method for the preparation of ultrathin fibers.* Angewandte Chemie International Edition, 2007. **46**(30): p. 5670-5703.
3. Reneker, D.H. and A.L. Yarin, *Electrospinning jets and polymer nanofibers.* Polymer, 2008. **49**(10): p. 2387-2425.
4. Kiyohiko, H., *Process for manufacturing artificial silk and other filaments by applying electric current*. 1929, Google Patents.
5. Huang, Z.-M., et al., *A review on polymer nanofibers by electrospinning and their applications in nanocomposites.* Composites science and technology, 2003. **63**(15): p. 2223-2253.
6. Sill, T.J. and H.A. von Recum, *Electrospinning: applications in drug delivery and tissue engineering.* Biomaterials, 2008. **29**(13): p. 1989-2006.
7. Taylor, G. *Electrically driven jets*. in *Proceedings of the Royal Society of London A: Mathematical, Physical and Engineering Sciences*. 1969. The Royal Society.
8. Yarin, A., S. Koombhongse, and D.H. Reneker, *Bending instability in electrospinning of nanofibers.* Journal of Applied Physics, 2001. **89**(5): p. 3018-3026.

9. Doshi, J. and D.H. Reneker. *Electrospinning process and applications of electrospun fibers*. in *Industry Applications Society Annual Meeting, 1993., Conference Record of the 1993 IEEE*. 1993. IEEE.

10. Yang, Q., et al., *Influence of solvents on the formation of ultrathin uniform poly (vinyl pyrrolidone) nanofibers with electrospinning.* Journal of Polymer Science Part B: Polymer Physics, 2004. **42**(20): p. 3721-3726.

11. Shin, Y., et al., *Electrospinning: A whipping fluid jet generates submicron polymer fibers.* Applied physics letters, 2001. **78**(8): p. 1149-1151.

12. Jaeger, R., et al. *Electrospinning of ultra-thin polymer fibers*. in *Macromolecular symposia*. 1998. Wiley Online Library.

13. Carson, R., et al., *Factors influencing electrically sprayed liquids.* AIAA Journal, 1964. **2**(8): p. 1460-1461.

14. Buchko, C.J., et al., *Processing and microstructural characterization of porous biocompatible protein polymer thin films.* Polymer, 1999. **40**(26): p. 7397-7407.

15. Deitzel, J., et al., *The effect of processing variables on the morphology of electrospun nanofibers and textiles.* Polymer, 2001. **42**(1): p. 261-272.

16. Reneker, D.H. and I. Chun, *Nanometre diameter fibres of polymer, produced by electrospinning.* Nanotechnology, 1996. **7**(3): p. 216.

17. Zhang, C., et al., *Study on morphology of electrospun poly (vinyl alcohol) mats.* European polymer journal, 2005. **41**(3): p. 423-432.

18. Li, Z. and C. Wang, *Effects of working parameters on electrospinning*, in *One-Dimensional Nanostructures*. 2013, Springer. p. 15-28.

19. Megelski, S., et al., *Micro-and nanostructured surface morphology on electrospun polymer fibers.* Macromolecules, 2002. **35**(22): p. 8456-8466.

20. Zargham, S., et al., *The effect of flow rate on morphology and deposition area of electrospun nylon 6 nanofiber.* J Eng Fibers Fabr, 2012. **7**(4): p. 42-9.

21. Sukigara, S., et al., *Regeneration of Bombyx mori silk by electrospinning—part 1: processing parameters and geometric properties.* Polymer, 2003. **44**(19): p. 5721-5727.

22. Koski, A., K. Yim, and S. Shivkumar, *Effect of molecular weight on fibrous PVA produced by electrospinning.* Materials Letters, 2004. **58**(3): p. 493-497.

23. Lyons, J., C. Li, and F. Ko, *Melt-electrospinning part I: processing parameters and geometric properties.* Polymer, 2004. **45**(22): p. 7597-7603.

24. Larrondo, L. and R. St John Manley, *Electrostatic fiber spinning from polymer melts. I. Experimental observations on fiber formation and properties.* Journal of Polymer Science: Polymer Physics Edition, 1981. **19**(6): p. 909-920.

25. Baumgarten, P.K., *Electrostatic spinning of acrylic microfibers.* Journal of colloid and interface science, 1971. **36**(1): p. 71-79.

26. Ding, B., et al., *Preparation and characterization of a nanoscale poly (vinyl alcohol) fiber aggregate produced by an electrospinning method.* Journal of Polymer Science Part B: Polymer Physics, 2002. **40**(13): p. 1261-1268.

27. Inai, R., M. Kotaki, and S. Ramakrishna, *Structure and properties of electrospun PLLA single nanofibres.* Nanotechnology, 2005. **16**(2): p. 208.

28. Kim, K.-H., et al., *Biological efficacy of silk fibroin nanofiber membranes for guided bone regeneration.* Journal of biotechnology, 2005. **120**(3): p. 327-339.

29. Lee, J.S., et al., *Role of molecular weight of atactic poly (vinyl alcohol)(PVA) in the structure and properties of PVA nanofabric prepared by electrospinning.* Journal of Applied Polymer Science, 2004. **93**(4): p. 1638-1646.

30. Zong, X., et al., *Structure and process relationship of electrospun bioabsorbable nanofiber membranes.* Polymer, 2002. **43**(16): p. 4403-4412.

31. Hayati, I., A. Bailey, and T.F. Tadros, *Investigations into the mechanisms of electrohydrodynamic spraying of liquids: I. Effect of electric field and the environment on pendant drops and factors affecting the formation of stable jets and atomization.* Journal of Colloid and Interface Science, 1987. **117**(1): p. 205-221.

32. Fong, H., I. Chun, and D. Reneker, *Beaded nanofibers formed during electrospinning.* Polymer, 1999. **40**(16): p. 4585-4592.

33. Huang, C., et al., *Electrospun polymer nanofibres with small diameters.* Nanotechnology, 2006. **17**(6): p. 1558.

34. Tan, E., S. Ng, and C. Lim, *Tensile testing of a single ultrafine polymeric fiber.* Biomaterials, 2005. **26**(13): p. 1453-1456.

35. Liu, J., et al., *Electrospinning in compressed carbon dioxide: Hollow or open-cell fiber formation with a single nozzle configuration.* The Journal of Supercritical Fluids, 2010. **53**(1): p. 142-150.

36. Stitzel, J., et al., *Controlled fabrication of a biological vascular substitute.* Biomaterials, 2006. **27**(7): p. 1088-1094.

37. Zhou, Y., et al., *Fabrication and electrical characterization of polyaniline-based nanofibers with diameter below 30 nm.* Applied Physics Letters, 2003. **83**(18): p. 3800-3802.

38. Gupta, P. and G.L. Wilkes, *Some investigations on the fiber formation by utilizing a side-by-side bicomponent electrospinning approach.* Polymer, 2003. **44**(20): p. 6353-6359.

39. Townsend-Nicholson, A. and S.N. Jayasinghe, *Cell electrospinning: a unique biotechnique for encapsulating living organisms for generating active biological microthreads/scaffolds.* Biomacromolecules, 2006. **7**(12): p. 3364-3369.

40. Liao, I.-C., et al., *Sustained viral gene delivery through core-shell fibers.* Journal of Controlled Release, 2009. **139**(1): p. 48-55.

41. Saraf, A., et al., *Regulated non-viral gene delivery from coaxial electrospun fiber mesh scaffolds.* Journal of Controlled Release, 2010. **143**(1): p. 95-103.

42. Liao, I.-C. and K.W. Leong, *Efficacy of engineered FVIII-producing skeletal muscle enhanced by growth factor-releasing co-axial electrospun fibers.* Biomaterials, 2011. **32**(6): p. 1669-1677.

43. He, C.L., et al., *Coaxial electrospun poly (L-lactic acid) ultrafine fibers for sustained drug delivery.* Journal of Macromolecular Science, Part B, 2006. **45**(4): p. 515-524.

44. Huang, Z.M., et al., *Encapsulating drugs in biodegradable ultrafine fibers through co-axial electrospinning.* Journal of Biomedical Materials Research Part A, 2006. **77**(1): p. 169-179.

45. He, C.L., Z.M. Huang, and X.J. Han, *Fabrication of drug-loaded electrospun aligned fibrous threads for suture applications.* Journal of biomedical materials research Part A, 2009. **89**(1): p. 80-95.

46. Ding, B., et al., *Fabrication of blend biodegradable nanofibrous nonwoven mats via multi-jet electrospinning.* Polymer, 2004. **45**(6): p. 1895-1902.

47. Varesano, A., R.A. Carletto, and G. Mazzuchetti, *Experimental investigations on the multi-jet electrospinning process.* Journal of Materials Processing Technology, 2009. **209**(11): p. 5178-5185.

48. Theron, S., et al., *Multiple jets in electrospinning: experiment and modeling.* Polymer, 2005. **46**(9): p. 2889-2899.

49. Teo, W. and S. Ramakrishna, *Electrospun fibre bundle made of aligned nanofibres over two fixed points.* Nanotechnology, 2005. **16**(9): p. 1878.

50. Kim, G., Y.-S. Cho, and W.D. Kim, *Stability analysis for multi-jets electrospinning process modified with a cylindrical electrode.* European polymer journal, 2006. **42**(9): p. 2031-2038.

51. Hong, Y., et al., *Generating elastic, biodegradable polyurethane/poly (lactide-co-glycolide) fibrous sheets with controlled antibiotic release via two-stream electrospinning.* Biomacromolecules, 2008. **9**(4): p. 1200-1207.

52. Persano, L., et al., *Industrial upscaling of electrospinning and applications of polymer nanofibers: a review.* Macromolecular Materials and Engineering, 2013. **298**(5): p. 504-520.

53. Gupta, B., N. Revagade, and J. Hilborn, *Poly (lactic acid) fiber: an overview.* Progress in polymer science, 2007. **32**(4): p. 455-482.

54. Cicero, J.A., et al., *Effects of molecular architecture on two-step, melt-spun poly (lactic acid) fibers.* Journal of Applied Polymer Science, 2002. **86**(11): p. 2839-2846.

55. Kim, M.S., J.C. Kim, and Y.H. Kim, *Effects of take-up speed on the structure and properties of melt-spun poly (L-lactic acid) fibers.* Polymers for Advanced Technologies, 2008. **19**(7): p. 748-755.

56. Postema, A., A. Luiten, and A. Pennings, *High-strength poly (L-lactide) fibers by a dry-spinning/hot-drawing process. I. Influence of the ambient temperature on the dry-spinning process.* Journal of applied polymer science, 1990. **39**(6): p. 1265-1274.

57. Wang, X., et al., *Formation of water-resistant hyaluronic acid nanofibers by blowing-assisted electro-spinning and non-toxic post treatments.* Polymer, 2005. **46**(13): p. 4853-4867.

58. Sundaray, B., et al., *Electrospinning of continuous aligned polymer fibers.* Applied physics letters, 2004. **84**(7): p. 1222-1224.

59. Li, D., Y. Wang, and Y. Xia, *Electrospinning nanofibers as uniaxially aligned arrays and layer-by-layer stacked films.* Advanced Materials, 2004. **16**(4): p. 361-366.

60. Ki, C.S., et al., *Electrospun three-dimensional silk fibroin nanofibrous scaffold.* Journal of applied polymer science, 2007. **106**(6): p. 3922-3928.

61. Smit, E., U. Bűttner, and R.D. Sanderson, *Continuous yarns from electrospun fibers.* Polymer, 2005. **46**(8): p. 2419-2423.

62. Xu, C., et al., *Aligned biodegradable nanofibrous structure: a potential scaffold for blood vessel engineering.* Biomaterials, 2004. **25**(5): p. 877-886.

63. Bazilevsky, A.V., A.L. Yarin, and C.M. Megaridis, *Co-electrospinning of core-shell fibers using a single-nozzle technique.* Langmuir, 2007. **23**(5): p. 2311-2314.

64. Bhattarai, N., et al., *Electrospun chitosan-based nanofibers and their cellular compatibility.* Biomaterials, 2005. **26**(31): p. 6176-6184.

65. Theron, A., E. Zussman, and A. Yarin, *Electrostatic field-assisted alignment of electrospun nanofibres.* Nanotechnology, 2001. **12**(3): p. 384.

66. Kilic, A., F. Oruc, and A. Demir, *Effects of polarity on electrospinning process.* Textile Research Journal, 2008. **78**(6): p. 532-539.

67. Zeng, J., et al., *Influence of the drug compatibility with polymer solution on the release kinetics of electrospun fiber formulation.* Journal of controlled release, 2005. **105**(1): p. 43-51.

68. Meng, Z., et al., *Preparation and characterization of electrospun PLGA/gelatin nanofibers as a potential drug delivery system.* Colloids and Surfaces B: Biointerfaces, 2011. **84**(1): p. 97-102.

69. Kim, K., et al., *Incorporation and controlled release of a hydrophilic antibiotic using poly (lactide-co-glycolide)-based electrospun nanofibrous scaffolds.* Journal of Controlled Release, 2004. **98**(1): p. 47-56.

70. Jannesari, M., et al., *Composite poly (vinyl alcohol)/poly (vinyl acetate) electrospun nanofibrous mats as a novel wound dressing matrix for controlled release of drugs.* Int J Nanomedicine, 2011. **6**: p. 993-1003.

71. Nair, R., et al., *Recent advances in solid lipid nanoparticle based drug delivery systems.* Journal of Biomedical Sciences and Research, 2011. **3**(2): p. 368-384.

72. Mickova, A., et al., *Core/shell nanofibers with embedded liposomes as a drug delivery system.* Biomacromolecules, 2012. **13**(4): p. 952-962.

73. Volpato, F.Z., et al., *Preservation of FGF-2 bioactivity using heparin-based nanoparticles, and their delivery from electrospun chitosan fibers.* Acta biomaterialia, 2012. **8**(4): p. 1551-1559.

74. Kim, H.S. and H.S. Yoo, *MMPs-responsive release of DNA from electrospun nanofibrous matrix for local gene therapy: in vitro and in vivo evaluation.* Journal of Controlled Release, 2010. **145**(3): p. 264-271.

75. Mottaghitalab, F., et al., *Enhancement of neural cell lines proliferation using nano-structured chitosan/poly (vinyl alcohol) scaffolds conjugated with nerve growth factor.* Carbohydrate Polymers, 2011. **86**(2): p. 526-535.

76. Choi, J.S., K.W. Leong, and H.S. Yoo, *In vivo wound healing of diabetic ulcers using electrospun nanofibers immobilized with human epidermal growth factor (EGF).* Biomaterials, 2008. **29**(5): p. 587-596.

77. Im, J.S., et al., *Fluorination of electrospun hydrogel fibers for a controlled release drug delivery system.* Acta biomaterialia, 2010. **6**(1): p. 102-109.

78. Yun, J., et al., *Electro-responsive transdermal drug delivery behavior of PVA/PAA/MWCNT nanofibers.* European Polymer Journal, 2011. **47**(10): p. 1893-1902.

79. Kim, H. and H. Yoo, *Matrix metalloproteinase-inspired suicidal treatments of diabetic ulcers with siRNA-decorated nanofibrous meshes.* Gene therapy, 2013. **20**(4): p. 378-385.

80. Luu, Y., et al., *Development of a nanostructured DNA delivery scaffold via electrospinning of PLGA and PLA–PEG block copolymers.* Journal of controlled release, 2003. **89**(2): p. 341-353.

81. Zamani, M., M.P. Prabhakaran, and S. Ramakrishna, *Advances in drug delivery via electrospun and electrosprayed nanomaterials.* Int J Nanomedicine, 2013. **8**(1): p. 2997-3017.

82. Xu, X., et al., *Ultrafine medicated fibers electrospun from W/O emulsions.* Journal of Controlled Release, 2005. **108**(1): p. 33-42.

83. Yang, Y., et al., *Release pattern and structural integrity of lysozyme encapsulated in core–sheath structured poly (DL-lactide) ultrafine fibers prepared by emulsion electrospinning.* European Journal of Pharmaceutics and Biopharmaceutics, 2008. **69**(1): p. 106-116.

84. He, S., et al., *Multiple release of polyplexes of plasmids VEGF and bFGF from electrospun fibrous scaffolds towards regeneration of mature blood vessels.* Acta biomaterialia, 2012. **8**(7): p. 2659-2669.

85. Yang, Y., et al., *Core–sheath structured fibers with pDNA polyplex loadings for the optimal release profile and transfection efficiency as potential tissue engineering scaffolds.* Acta biomaterialia, 2011. **7**(6): p. 2533-2543.

86. Yang, Y., et al., *Promotion of skin regeneration in diabetic rats by electrospun core-sheath fibers loaded with basic fibroblast growth factor.* Biomaterials, 2011. **32**(18): p. 4243-4254.

87. Wang, Y., W. Qiao, and T. Yin, *A novel controlled release drug delivery system for multiple drugs based on electrospun nanofibers containing nanoparticles.* Journal of pharmaceutical sciences, 2010. **99**(12): p. 4805-4811.

88. Xu, J., et al., *Controlled dual release of hydrophobic and hydrophilic drugs from electrospun poly (l-lactic acid) fiber mats loaded with chitosan microspheres.* Materials letters, 2011. **65**(17): p. 2800-2803.

89. Okuda, T., K. Tominaga, and S. Kidoaki, *Time-programmed dual release formulation by multilayered drug-loaded nanofiber meshes.* Journal of Controlled Release, 2010. **143**(2): p. 258-264.

90. Chunder, A., et al., *Fabrication of ultrathin polyelectrolyte fibers and their controlled release properties.* Colloids and Surfaces B: Biointerfaces, 2007. **58**(2): p. 172-179.

91. Im, J.S., et al., *Prediction and characterization of drug release in a multi-drug release system.* Journal of Industrial and Engineering Chemistry, 2012. **18**(1): p. 325-330.

92. Prausnitz, M.R. and R. Langer, *Transdermal drug delivery.* Nature biotechnology, 2008. **26**(11): p. 1261-1268.

93. Suwantong, O., U. Ruktanonchai, and P. Supaphol, *Electrospun cellulose acetate fiber mats containing asiaticoside or Centella asiatica crude extract and the release characteristics of asiaticoside.* Polymer, 2008. **49**(19): p. 4239-4247.

94. Taepaiboon, P., U. Rungsardthong, and P. Supaphol, *Drug-loaded electrospun mats of poly (vinyl alcohol) fibres and their release characteristics of four model drugs.* Nanotechnology, 2006. **17**(9): p. 2317.

95. Suwantong, O., et al., *Electrospun cellulose acetate fiber mats containing curcumin and release characteristic of the herbal substance.* Polymer, 2007. **48**(26): p. 7546-7557.

96. Im, J.S., B.C. Bai, and Y.-S. Lee, *The effect of carbon nanotubes on drug delivery in an electro-sensitive transdermal drug delivery system.* Biomaterials, 2010. **31**(6): p. 1414-1419.

97. Taepaiboon, P., U. Rungsardthong, and P. Supaphol, *Vitamin-loaded electrospun cellulose acetate nanofiber mats as transdermal and dermal therapeutic agents of vitamin A acid and vitamin E.* European Journal of Pharmaceutics and Biopharmaceutics, 2007. **67**(2): p. 387-397.

98. Ngawhirunpat, T., et al., *Development of meloxicam-loaded electrospun polyvinyl alcohol mats as a transdermal therapeutic agent.* Pharmaceutical development and technology, 2009. **14**(1): p. 73-82.

99. Kenawy, E.-R., et al., *Release of tetracycline hydrochloride from electrospun poly (ethylene-co-vinylacetate), poly (lactic acid), and a blend.* Journal of controlled release, 2002. **81**(1): p. 57-64.

100. Wang, X., T. Yue, and T.-c. Lee, *Development of Pleurocidin-poly (vinyl alcohol) electrospun antimicrobial nanofibers to retain antimicrobial activity in food system application.* Food Control, 2015. **54**: p. 150-157.

101. Zhang, Y., et al., *Recent development of polymer nanofibers for biomedical and biotechnological applications.* Journal of Materials Science: Materials in Medicine, 2005. **16**(10): p. 933-946.

102. Tian, L., et al., *Emulsion electrospun vascular endothelial growth factor encapsulated poly (l-lactic acid-co-ε-caprolactone) nanofibers for sustained release in cardiac tissue engineering.* Journal of Materials Science, 2012. **47**(7): p. 3272-3281.

103. Boateng, J.S., et al., *Wound healing dressings and drug delivery systems: a review.* Journal of pharmaceutical sciences, 2008. **97**(8): p. 2892-2923.

104. Said, S.S., et al., *Antimicrobial PLGA ultrafine fibers: Interaction with wound bacteria.* European Journal of Pharmaceutics and Biopharmaceutics, 2011. **79**(1): p. 108-118.

105. Thakur, R., et al., *Electrospun nanofibrous polymeric scaffold with targeted drug release profiles for potential application as wound dressing.* International journal of pharmaceutics, 2008. **364**(1): p. 87-93.

106. Wang, A., et al., *Experimental investigation of the properties of electrospun nanofibers for potential medical application.* Journal of Nanomaterials, 2015. **2015**: p. 5.

107. GhavamiNejad, A., et al., *Mussel-inspired electrospun nanofibers functionalized with size-controlled silver nanoparticles for wound dressing application.* ACS applied materials & interfaces, 2015. **7**(22): p. 12176-12183.

108. Ignatova, M., I. Rashkov, and N. Manolova, *Drug-loaded electrospun materials in wound-dressing applications and in local cancer treatment.* Expert opinion on drug delivery, 2013. **10**(4): p. 469-483.

109. Chutipakdeevong, J., U. Ruktanonchai, and P. Supaphol, *Hybrid biomimetic electrospun fibrous mats derived from poly (ε-caprolactone) and silk fibroin protein for wound dressing application.* Journal of Applied Polymer Science, 2015. **132**(11).

110. Xu, X., et al., *The release behavior of doxorubicin hydrochloride from medicated fibers prepared by emulsion-electrospinning.* European Journal of Pharmaceutics and Biopharmaceutics, 2008. **70**(1): p. 165-170.

111. Xu, X., et al., *Ultrafine PEG–PLA fibers loaded with both paclitaxel and doxorubicin hydrochloride and their in vitro cytotoxicity.* European Journal of Pharmaceutics and Biopharmaceutics, 2009. **72**(1): p. 18-25.

112. Xie, J., R.S. Tan, and C.H. Wang, *Biodegradable microparticles and fiber fabrics for sustained delivery of cisplatin to treat C6 glioma in vitro.* Journal of Biomedical Materials Research Part A, 2008. **85**(4): p. 897-908.

113. Lee, M.H., et al., *Exovascular application of epigallocatechin-3-O-gallate-releasing electrospun poly (l-lactide glycolic acid) fiber sheets to reduce intimal hyperplasia in injured abdominal aorta.* Biomedical Materials, 2015. **10**(5): p. 055010.

114. Liu, S., et al., *Inhibition of orthotopic secondary hepatic carcinoma in mice by doxorubicin-loaded electrospun polylactide nanofibers.* 2013.

115. Luo, X., et al., *Antitumor activities of emulsion electrospun fibers with core loading of hydroxycamptothecin via intratumoral implantation.* International journal of pharmaceutics, 2012. **425**(1): p. 19-28.

116. Chen, P., et al., *A controlled release system of titanocene dichloride by electrospun fiber and its antitumor activity in vitro.* European Journal of Pharmaceutics and Biopharmaceutics, 2010. **76**(3): p. 413-420.

117. Shao, S., et al., *Controlled green tea polyphenols release from electrospun PCL/MWCNTs composite nanofibers.* International journal of pharmaceutics, 2011. **421**(2): p. 310-320.

118. Chew, S.Y., et al., *Sustained release of proteins from electrospun biodegradable fibers.* Biomacromolecules, 2005. **6**(4): p. 2017-2024.

119. Rujitanaroj, P.-o., et al., *Nanofiber-mediated controlled release of siRNA complexes for long term gene-silencing applications.* Biomaterials, 2011. **32**(25): p. 5915-5923.

120. Cao, H., et al., *RNA interference by nanofiber-based siRNA delivery system.* Journal of Controlled Release, 2010. **144**(2): p. 203-212.

121. Schneider, A., et al., *Biofunctionalized electrospun silk mats as a topical bioactive dressing for accelerated wound healing.* Acta Biomaterialia, 2009. **5**(7): p. 2570-2578.

122. Zhang, X., et al., *In vitro biocompatibility study of electrospun copolymer ethylene carbonate-ε-caprolactone and vascular endothelial growth factor blended nanofibrous scaffolds.* Applied Surface Science, 2012. **258**(7): p. 2301-2306.

123. Chen, M., et al., *Chitosan/siRNA nanoparticles encapsulated in PLGA nanofibers for siRNA delivery.* ACS nano, 2012. **6**(6): p. 4835-4844.

124. Cho, Y.I., et al., *Nerve growth factor (NGF)-conjugated electrospun nanostructures with topographical cues for neuronal differentiation of mesenchymal stem cells.* Acta biomaterialia, 2010. **6**(12): p. 4725-4733.

125. Han, N., et al., *Hydrogel–electrospun fiber composite materials for hydrophilic protein release.* Journal of controlled release, 2012. **158**(1): p. 165-170.

126. Chen, G. and Y. Lv, *Immobilization and application of electrospun nanofiber scaffold-based growth factor in bone tissue engineering.* Current pharmaceutical design, 2015. **21**(15): p. 1967-1978.

127. Zahedi, P., et al., *Preparation and performance evaluation of tetracycline hydrochloride loaded wound dressing mats based on electrospun nanofibrous poly (lactic acid)/poly (ϵ-caprolactone) blends.* Journal of Applied Polymer Science, 2012. **124**(5): p. 4174-4183.

128. Gilchrist, S.E., et al., *Fusidic acid and rifampicin co-loaded PLGA nanofibers for the prevention of orthopedic implant associated infections.* Journal of Controlled Release, 2013. **170**(1): p. 64-73.

129. Zamani, M., et al., *Controlled release of metronidazole benzoate from poly ε-caprolactone electrospun nanofibers for periodontal diseases.* European Journal of Pharmaceutics and Biopharmaceutics, 2010. **75**(2): p. 179-185.

130. Toncheva, A., et al., *Antibacterial fluoroquinolone antibiotic-containing fibrous materials from poly (l-lactide-co-d, l-lactide) prepared by electrospinning.* European Journal of Pharmaceutical Sciences, 2012. **47**(4): p. 642-651.

131. Spasova, M., et al., *Preparation of chitosan-containing nanofibres by electrospinning of chitosan/poly (ethylene oxide) blend solutions.* e-Polymers, 2004. **4**(1): p. 624-635.

132. Verreck, G., et al., *Incorporation of drugs in an amorphous state into electrospun nanofibers composed of a water-insoluble, nonbiodegradable polymer.* Journal of Controlled Release, 2003. **92**(3): p. 349-360.

133. Huang, L.-Y., et al., *Time-engineeringed biphasic drug release by electrospun nanofiber meshes.* International journal of pharmaceutics, 2012. **436**(1): p. 88-96.

134. Jiang, H., et al., *Preparation and characterization of ibuprofen-loaded poly (lactide-co-glycolide)/poly (ethylene glycol)-g-chitosan electrospun membranes.* Journal of Biomaterials Science, Polymer Edition, 2004. **15**(3): p. 279-296.

135. Jiang, Y.-N., H.-Y. Mo, and D.-G. Yu, *Electrospun drug-loaded core–sheath PVP/zein nanofibers for biphasic drug release.* International journal of pharmaceutics, 2012. **438**(1): p. 232-239.

136. Chew, S.Y., et al., *Aligned Protein–Polymer Composite Fibers Enhance Nerve Regeneration: A Potential Tissue-Engineering Platform.* Advanced functional materials, 2007. **17**(8): p. 1288-1296.

137. Kowalczyk, T., et al., *Electrospinning of bovine serum albumin. Optimization and the use for production of biosensors.* Biomacromolecules, 2008. **9**(7): p. 2087-2090.

138. Li, X., et al., *Encapsulation of proteins in poly (l-lactide-co-caprolactone) fibers by emulsion electrospinning.* Colloids and Surfaces B: Biointerfaces, 2010. **75**(2): p. 418-424.

139. Lu, T., et al., *Doxorubicin-loaded ultrafine PEG-PLA fiber mats against hepatocarcinoma.* Journal of Applied Polymer Science, 2012. **123**(1): p. 209-217.

140. Ranganath, S.H. and C.-H. Wang, *Biodegradable microfiber implants delivering paclitaxel for post-surgical chemotherapy against malignant glioma.* Biomaterials, 2008. **29**(20): p. 2996-3003.

141. Xie, J. and C.-H. Wang, *Electrospun micro-and nanofibers for sustained delivery of paclitaxel to treat C6 glioma in vitro.* Pharmaceutical research, 2006. **23**(8): p. 1817-1826.

142. Liu, D., et al., *Necrosis of cervical carcinoma by dichloroacetate released from electrospun polylactide mats.* Biomaterials, 2012. **33**(17): p. 4362-4369.

143. Xu, X., et al., *Preparation of core-sheath composite nanofibers by emulsion electrospinning.* Macromolecular Rapid Communications, 2006. **27**(19): p. 1637-1642.

144. Huang, L., R.P. Apkarian, and E.L. Chaikof, *High-resolution analysis of engineered type I collagen nanofibers by electron microscopy.* Scanning, 2001. **23**(6): p. 372-375.

145. Huang, L., et al., *Engineered collagen–PEO nanofibers and fabrics.* Journal of biomaterials science, Polymer edition, 2001. **12**(9): p. 979-993.

146. Zhang, E., et al., *Electrospun PDLLA/PLGA composite membranes for potential application in guided tissue regeneration.* Materials Science and Engineering: C, 2016. **58**: p. 278-285.

147. Pal Kaur, I. and M. Kanwar, *Ocular preparations: the formulation approach.* Drug development and industrial pharmacy, 2002. **28**(5): p. 473-493.

148. HS Boddu, S., *Polymeric Nanoparticles for Ophthalmic Drug Delivery: An Update on Research and Patenting Activity.* Recent Patents on Nanomedicine, 2012. **2**(2): p. 96-112.

149. Le Bourlais, C., et al., *Ophthalmic drug delivery systems—recent advances.* Progress in retinal and eye research, 1998. **17**(1): p. 33-58.

150. Schoenwald, R. and P. Stewart, *Effect of particle size on ophthalmic bioavailability of dexamethasone suspensions in rabbits.* Journal of pharmaceutical sciences, 1980. **69**(4): p. 391-394.

151. Srivastava, R. and K. Pathak, *An updated patent review on ocular drug delivery systems with potential for commercial viability.* Recent patents on drug delivery & formulation, 2011. **5**(2): p. 146-162.

152. Gaudana, R., et al., *Ocular drug delivery.* The AAPS journal, 2010. **12**(3): p. 348-360.

153. Bucolo, C., F. Drago, and S. Salomone, *Ocular drug delivery: a clue from nanotechnology.* Frontiers in pharmacology, 2012. **3**: p. 188.

154. Prausnitz, M.R. and J.S. Noonan, *Permeability of cornea, sclera, and conjunctiva: a literature analysis for drug delivery to the eye.* Journal of pharmaceutical sciences, 1998. **87**(12): p. 1479-1488.

155. Huang, H.S., R.D. Schoenwald, and J.L. Lach, *Corneal penetration behavior of β-blocking agents II: Assessment of barrier contributions.* Journal of pharmaceutical sciences, 1983. **72**(11): p. 1272-1279.

156. Schoenwald, R.D. and R.L. Ward, *Relationship between steroid permeability across excised rabbit cornea and octanol-water partition coefficients.* Journal of pharmaceutical sciences, 1978. **67**(6): p. 786-788.

157. Saettone, M.F., B. Giannaccini, and D. Monti, *Ophthalmic emulsions and suspensions.* Journal of Toxicology: Cutaneous and Ocular Toxicology, 2001. **20**(2-3): p. 183-201.

158. Smolin, G., et al., *Idoxuridine-liposome therapy for herpes simplex keratitis.* American journal of ophthalmology, 1981. **91**(2): p. 220-225.

159. Gupta, H., et al., *Sparfloxacin-loaded PLGA nanoparticles for sustained ocular drug delivery.* Nanomedicine: nanotechnology, biology and medicine, 2010. **6**(2): p. 324-333.

160. Lee, V.H. and J.R. Robinson, *Topical ocular drug delivery: recent developments and future challenges.* Journal of ocular pharmacology and therapeutics, 1986. **2**(1): p. 67-108.

161. Cohen, E.M., *Dexamethasone*, in *Analytical Profiles of Drug Substances*, F. Klaus, Editor. 1973, Academic Press. p. 163-197.

162. Wang, J.D., et al., *Quantitative analysis of molecular absorption into PDMS microfluidic channels.* Annals of biomedical engineering, 2012. **40**(9): p. 1862-1873.

163. Barnes, P.J., *Anti-inflammatory actions of glucocorticoids: molecular mechanisms.* Clinical science, 1998. **94**(6): p. 557-572.

164. Thompson, E.B. and M.E. Lippman, *Mechanism of action of glucocorticoids.* Metabolism, 1974. **23**(2): p. 159-202.

165. Rhen, T. and J.A. Cidlowski, *Antiinflammatory action of glucocorticoids—new mechanisms for old drugs.* New England Journal of Medicine, 2005. **353**(16): p. 1711-1723.

166. Vane, J. and R. Botting, *New insights into the mode of action of anti-inflammatory drugs.* Inflammation Research, 1995. **44**(1): p. 1-10.

167. Gordon, D.M., *Use of dexamethasone in eye disease.* Journal of the American Medical Association, 1960. **172**(4): p. 311-312.

168. *Maxidex Package Insert*. 2003, Food and Drug Administration.

169. Cronau, H., R.R. Kankanala, and T. Mauger, *Diagnosis and management of red eye in primary care.* Am Fam Physician, 2010. **81**(2): p. 137-144.

170. Winfield, A., et al., *A study of the causes of non-compliance by patients prescribed eyedrops.* British Journal of Ophthalmology, 1990. **74**(8): p. 477-480.

171. Gan, L., et al., *Self-assembled liquid crystalline nanoparticles as a novel ophthalmic delivery system for dexamethasone: improving preocular retention and ocular bioavailability.* International journal of pharmaceutics, 2010. **396**(1): p. 179-187.

172. Greaves, J., C. Wilson, and A. Birmingham, *Assessment of the precorneal residence of an ophthalmic ointment in healthy subjects.* British journal of clinical pharmacology, 1993. **35**(2): p. 188.

173. Urtti, A. and L. Salminen, *Minimizing systemic absorption of topically administered ophthalmic drugs.* Survey of ophthalmology, 1993. **37**(6): p. 435-456.

174. Chrai, S.S., et al., *Lacrimal and instilled fluid dynamics in rabbit eyes.* Journal of pharmaceutical sciences, 1973. **62**(7): p. 1112-1121.

175. Patton, T.F. and J.R. Robinson, *Quantitative precorneal disposition of topically applied pilocarpine nitrate in rabbit eyes.* Journal of pharmaceutical sciences, 1976. **65**(9): p. 1295-1301.

176. Kim, J. and A. Chauhan, *Dexamethasone transport and ocular delivery from poly (hydroxyethyl methacrylate) gels.* International journal of pharmaceutics, 2008. **353**(1): p. 205-222.

177. Fialho, S.L. and D. Silva-Cunha, *New vehicle based on a microemulsion for topical ocular administration of dexamethasone.* Clinical & experimental ophthalmology, 2004. **32**(6): p. 626-632.

178. Cholkar, K., et al., *Novel nanomicellar formulation approaches for anterior and posterior segment ocular drug delivery.* Recent patents on nanomedicine, 2012. **2**(2): p. 82.

179. Cholkar, K., et al., *Optimization of dexamethasone mixed nanomicellar formulation.* AAPS PharmSciTech, 2014. **15**(6): p. 1454-1467.

180. Patel, S., et al., *Development and evaluation of dexamethasone nanomicelles with potential for treating posterior uveitis after topical application.* Journal of Ocular Pharmacology and Therapeutics, 2015. **31**(4): p. 215-227.

181. Weijtens, O., et al., *Peribulbar corticosteroid injection: vitreal and serum concentrations after dexamethasone disodium phosphate injection.* American journal of ophthalmology, 1997. **123**(3): p. 358-363.

182. Baeyens, V., et al., *Optimized release of dexamethasone and gentamicin from a soluble ocular insert for the treatment of external ophthalmic infections.* Journal of controlled release, 1998. **52**(1): p. 215-220.

183. Kumari, A., et al., *Ocular inserts-Advancement in therapy of eye diseases.* Journal of advanced pharmaceutical technology & research, 2010. **1**(3): p. 291.

184. Franca, J.R., et al., *Bimatoprost-loaded ocular inserts as sustained release drug delivery systems for glaucoma treatment: in vitro and in vivo evaluation.* PloS one, 2014. **9**(4): p. e95461.

185. Kawakami, S., et al., *Controlled release and ocular absorption of tilisolol utilizing ophthalmic insert-incorporated lipophilic prodrugs.* Journal of controlled release, 2001. **76**(3): p. 255-263.

186. Aburahma, M.H. and A.A. Mahmoud, *Biodegradable ocular inserts for sustained delivery of brimonidine tartarate: preparation and in vitro/in vivo evaluation.* Aaps Pharmscitech, 2011. **12**(4): p. 1335-1347.

187. B Gevariya, H. and J. K Patel, *Long acting betaxolol ocular inserts based on polymer composite.* Current drug delivery, 2013. **10**(4): p. 384-393.

188. Hornof, M., et al., *Mucoadhesive ocular insert based on thiolated poly (acrylic acid): development and in vivo evaluation in humans.* Journal of Controlled Release, 2003. **89**(3): p. 419-428.

189. Mckee, J.T.J.K.J.H.Y., *Ocular drug delivery devices*, W.I.P. Organization, Editor. 2011, Aton Pharma, Inc. Louisiana State University Agricultural And Mechanical College.

190. Zahedi, P., et al., *A review on wound dressings with an emphasis on electrospun nanofibrous polymeric bandages.* Polymers for Advanced Technologies, 2010. **21**(2): p. 77-95.

191. Zhou, H., A.H. Touny, and S.B. Bhaduri, *Fabrication of novel PLA/CDHA bionanocomposite fibers for tissue engineering applications via electrospinning.* Journal of Materials Science: Materials in Medicine, 2011. **22**(5): p. 1183-1193.

192. Touny, A.H., et al., *Effect of electrospinning parameters on the characterization of PLA/HNT nanocomposite fibers.* Journal of Materials Research, 2010. **25**(05): p. 857-865.

193. Touny, A.H. and S.B. Bhaduri, *A reactive electrospinning approach for nanoporous PLA/monetite nanocomposite fibers.* Materials Science and Engineering: C, 2010. **30**(8): p. 1304-1312.

194. Zhou, H., et al., *Fabrication of novel poly (lactic acid)/amorphous magnesium phosphate bionanocomposite fibers for tissue engineering applications via electrospinning.* Materials Science and Engineering: C, 2013. **33**(4): p. 2302-2310.

195. Manvi, F., et al., *Formulation of a transdermal drug delivery system of ketotifen fumarate.* Indian journal of pharmaceutical sciences, 2003. **65**(3): p. 239-243.

196. Khairnar, A., et al., *Developmement of mucoadhesive buccal patch containing aceclofenac: in vitro evaluations.* Int. J. PharmTech Res, 2009. **1**(4): p. 978-981.

197. Singh Malik, D., N. Mital, and G. Kaur, *Topical drug delivery systems: a patent review.* Expert opinion on therapeutic patents, 2016. **26**(2): p. 213-228.

198. Al-Saedi, Z.H., R.M. Alzhrani, and S.H. Boddu, *Formulation and In Vitro Evaluation of Cyclosporine-A Inserts Prepared Using Hydroxypropyl Methylcellulose for Treating Dry Eye Disease.* Journal of Ocular Pharmacology and Therapeutics, 2016.

199. Zhang, M., et al., *Properties and biocompatibility of chitosan films modified by blending with PEG.* Biomaterials, 2002. **23**(13): p. 2641-2648.

200. Efron, N., G. Young, and N.A. Brennan, *Ocular surface temperature.* Current eye research, 1989. **8**(9): p. 901-906.

201. Scott, J.A., *A finite element model of heat transport in the human eye.* Physics in Medicine and Biology, 1988. **33**(2): p. 227.

202. Gottlieb, H.E., V. Kotlyar, and A. Nudelman, *NMR chemical shifts of common laboratory solvents as trace impurities.* The Journal of organic chemistry, 1997. **62**(21): p. 7512-7515.

203. MacCallum, D.K., et al., *Bovine corneal endothelium in vitro: elaboration and organization of a basement membrane.* Experimental cell research, 1982. **139**(1): p. 1-13.

204. Nesamony, J., et al., *Development and characterization of nanostructured mists with potential for actively targeting poorly water-soluble compounds into the lungs.* Pharmaceutical research, 2013. **30**(10): p. 2625-2639.

205. Rodrigues, L.B., et al., *In vitro release and characterization of chitosan films as dexamethasone carrier.* International journal of pharmaceutics, 2009. **368**(1): p. 1-6.

206. Garlotta, D., *A literature review of poly (lactic acid).* Journal of Polymers and the Environment, 2001. **9**(2): p. 63-84.

207. Sudhamani, S., M. Prasad, and K.U. Sankar, *DSC and FTIR studies on gellan and polyvinyl alcohol (PVA) blend films.* Food Hydrocolloids, 2003. **17**(3): p. 245-250.

208. Gómez-Gaete, C., et al., *Encapsulation of dexamethasone into biodegradable polymeric nanoparticles.* International journal of pharmaceutics, 2007. **331**(2): p. 153-159.

209. Silverajah, V., et al., *A comparative study on the mechanical, thermal and morphological characterization of poly (lactic acid)/epoxidized palm oil blend.* International journal of molecular sciences, 2012. **13**(5): p. 5878-5898.

210. Hassan, C.M. and N.A. Peppas, *Structure and Morphology of Freeze/Thawed PVA Hydrogels.* Macromolecules, 2000. **33**(7): p. 2472-2479.

211. Wang, Y., et al., *Preparation and characterization of polylactide/poly (ε-caprolactone)-poly (ethylene glycol)-poly (ε-caprolactone) hybrid fibers for potential application in bone tissue engineering.* Int J Nanomedicine, 2014. **9**: p. 1991-2003.

212. Teixeira, E.d.M., et al., *Starch/fiber/poly (lactic acid) foam and compressed foam composites.* RSC Advances, 2014. **4**(13): p. 6616-6623.

213. Santos, F.A.d. and M.I.B. Tavares, *Development and characterization of hybrid materials based on biodegradable PLA matrix, microcrystalline cellulose and organophilic silica.* Polímeros, 2014. **24**(5): p. 561-566.

214. Rathna, G.V.N., J.P. Jog, and A.B. Gaikwad, *Development of non-woven nanofibers of egg albumen-poly (vinyl alcohol) blends: influence of solution properties on morphology of nanofibers.* Polymer journal, 2011. **43**(7): p. 654-661.

215. Ma, H., T. Shi, and Q. Song, *Synthesis and Characterization of Novel PVA/SiO2-TiO2 Hybrid Fibers.* Fibers, 2014. **2**(4): p. 275-284.

216. Midelfart, A., A. Dybdahl, and J. Krane, *Detection of dexamethasone in the cornea and lens by NMR spectroscopy.* Graefe's archive for clinical and experimental ophthalmology, 1999. **237**(5): p. 415-423.

217. Kim, J., A. Conway, and A. Chauhan, *Extended delivery of ophthalmic drugs by silicone hydrogel contact lenses.* Biomaterials, 2008. **29**(14): p. 2259-2269.

218. Peng, M., et al., *Porous poly (vinylidene fluoride) membrane with highly hydrophobic surface.* Journal of Applied Polymer Science, 2005. **98**(3): p. 1358-1363.

219. Saliba, J.B., et al., *Characterization and in vitro release of cyclosporine-A from poly (D, L-lactide-co-glycolide implants obtained by solvent/extraction evaporation.* Química Nova, 2012. **35**(4): p. 723-727.

220. Haider, A., S. Haider, and I.-K. Kang, *A comprehensive review summarizing the effect of electrospinning parameters and potential applications of nanofibers in biomedical and biotechnology.* Arabian Journal of Chemistry.

221. Petersson, L., I. Kvien, and K. Oksman, *Structure and thermal properties of poly (lactic acid)/cellulose whiskers nanocomposite materials.* Composites Science and Technology, 2007. **67**(11): p. 2535-2544.

222. Pastoriza-Santos, I. and L.M. Liz-Marzán, *Synthesis of silver nanoprisms in DMF.* Nano letters, 2002. **2**(8): p. 903-905.

223. Lynch, D., *NTP technical report on the toxicity studies of N, N-Dimethylformamide (CAS No. 68-12-2) Administered by Inhalation to F344/N Rats and B6C3F1 Mice.* Toxicity report series, 1992. **22**: p. 1-D20.

224. Kennedy, G.L., *Acute and Subchronic Toxicity of Dimethylformam Ide and Dimethylacetamide Following Various Routes of Administration.* Drug and chemical toxicology, 1986. **9**(2): p. 147-170.

225. Grant, W.M. and J.S. Schuman, *Toxicology of the eye: effects on the eyes and visual system from chemicals, drugs, metals and minerals, plants, toxins and venoms; also systemic side effects from eye medications*. Vol. 1. 1993: Charles C Thomas Publisher.

226. Grant, W.M., *Toxicology of the Eye*. 1962: Thomas.

227. Aldricha, D.S., et al., *Ophthalmic preparations.* 2013.